

学位論文（要約）

Bioluminescence Analysis and Optical Control of  
Phosphatidylinositol (3,4,5)-Triphosphate on the Cell  
Membrane

（細胞膜上ホスファチジルイノシトール  
3, 4, 5-三リン酸の生物発光分析と光制御法）

平成 25 年 12 月 博士（理学）申請  
東京大学大学院理学系研究科化学専攻

Yang Lingzhi

楊 靈芝

## Abstract

Phosphatidylinositol (3,4,5)- trisphosphate (PIP3) is a lipid second messenger which mediates central cellular events such as growth, motility and development by recruiting and activating downstream proteins. The PIP3 level in an un-stimulated cell is balanced between its synthesis by the phosphatidylinositol 3-kinase (PI3K) upon receptor stimulation and its degradation by lipid phosphatases. Loss of such equilibrium results in an elevation of PIP3 amount in tumorigenic cells or a suppression of PIP3 level which retards the growth of nerve cells. Although PIP3 abnormality is related to fatal diseases, the various roles of PIP3 have not been resolved thoroughly because of limitations of PIP3 analytical methods. Previous methods have used PIP3 antibodies, instrumental separation, or fluorescence imaging to analyze the PIP3. However, the in vitro immunoblotting and instrumental analysis involve cell demolishing sample pretreatment that may decompose the PIP3. Fluorescence imaging enables the visualization of PIP3 in living cells, however, the observation area is confined by a microscope and a plausible quantification is caused by the instability of a fluorescent protein. The spatiotemporal and quantitative analysis of PIP3, which is of critical importance to unveil the precise regulative roles of PIP3, remains difficult. In this study, we focus on the development of bioluminescent probes to analyze the relative amount of PIP3 using split luciferase complementation, and furthermore, on the establishment of an optical system to control the production of PIP3 on cellular membranes using light sensitive protein-protein interaction.

In chapter 1, the background and basic concepts for this study such as PIP3, bioluminescence analysis and light inducible protein-protein interactions are introduced.

In chapter 2, a scheme for PIP3 analysis using bioluminescent probes is proposed. A pair of split luciferase probes was developed to quantify the production of PIP3 on

the plasma membrane. In the scheme, a full-length luciferase is dissected into N- and C- terminal luciferase fragments and the luciferase activity is completely lost. When the two fragments approach each other with a close proximity, they reconstitute to recover the luciferase activity and produce the bioluminescence signal. The PIP3 probes using split luciferase fragments took advantage of a Pleckstrin Homology domain that specifically binds PIP3. Tandem PH domains are fused with a C-terminal luciferase fragment, expressed in the cytosol, whereas the N-terminal luciferase fragment is predominantly localized on the plasma membrane. In response to PIP3 production, PH domain would be brought to the plasma membrane by the PHD-PIP3 interactions and such interaction promotes the co-localization of two luciferase fragments. The co-localized fragments spontaneously reconstitute to form an active luciferase producing bioluminescence recovery. The bioluminescence signals are proportional to the amounts of PIP3 produced on the plasma membrane. The probes were used to bioluminescence imaging of PIP3 production and also used to establish a High Throughput Screening (HTS) system for PIP3 related compounds. The PIP3 probes provide important features including temporal recording of PIP3 production by bioluminescence and analysis of relative PIP3 amount on the plasma membrane with minimal cell toxicity. The study is based on a novel methodology of self-associative luciferase fragment complementation that enables further analyses of other lipid messengers with bioluminescence signals.

In chapter 3, a system for the optical control of PIP3 production is developed. PIP3 is a pivotal lipid messenger that plays various roles. Diverse functions are likely to be resulted from spatiotemporal effects of PIP3 naturally produced on specific cellular membranes. Therefore, we seek to establish a method to control the production of PIP3 on cell membranes at specific cellular localizations. Previously, PIP3 is synthesized upon ligand stimulation with low spatial specificity. In this study, to overcome limitations of the ligand stimulation by chemicals, an optogenetic system that uses light sensitive protein-protein interactions is developed to perturb the PIP3 production

spatiotemporally. *Arabidopsis* cryptochrome 2 (CRY2) interacts with CIBN protein with sub-second timescale when irradiated with blue light, whereas the CRY2 dissociates with CIBN when the CRY2-CIBN complex is kept in the dark or irradiated by red light. In order to control the PIP3 production, A CIBN is anchored on a subcellular membrane, whereas a CRY2 is fused with a constitutively active PI 3-kinase (acPI3K), which synthesizes PIP3, expressed in the cytosol. acPI3K would be recruited to the membrane after light stimulation by the light-gated CRY2-CIBN interaction. As PIP3 is synthesized on a specific cell membrane, its production is visualized by the localization of a PH domain, which specifically binds PIP3. Fluorescent proteins are fused with each construct to monitor the dynamics and cellular localizations of fusion proteins. The PIP3 was reversibly produced by blue light stimulation and cell movements were observed after the irradiation. This method clarifies a path for more extensive study of PIP3 functions.

In chapter 4, the concluding remarks are given. We developed probes for PIP3 analysis based on luciferase fragment complementation. A novel concept of self-associative luciferase fragment complementation is introduced for PIP3 analysis. The PIP3 probes provide important features including temporal recording of PIP3 production by bioluminescence and analysis of relative PIP3 amounts with minimal cell toxicity. We quantified agonist and inhibitor of PI 3-kinase that affected production of PIP3 on the plasma membrane and validated a high throughput screening system for PIP3 related reagents using the bioluminescent probes. We further monitored the PIP3 production by establishing an optogenetic system using light gated dimerization of CRY2 and CIB1. In substitution of chemical stimulation, the optogenetic system initiated PIP3 synthesis exclusively on the plasma membrane with reversibility. Efforts have also been made to examine the movements of cells in response to the blue light stimulation.

This study clarifies a path towards more extensive investigation of PIP3 and potentially other membrane lipid second messengers using luciferase fragment

complementation. The optogenetic system for PIP3 production is meaningful for studying the regulative roles of PIP3 on different cellular locations.

## Table of Contents

1.	General Introduction.....	1
1.1	Introduction of Phosphatidylinositol (3,4,5)- Trisphosphate (PIP3).....	1
1.1.1	General Features of PIP3.....	1
1.1.2	PIP3 Binding Modular Domains.....	5
1.1.3	Analytical Methods for PIP3.....	7
1.2	Introduction of Bioluminescence Analysis.....	11
1.2.1	Characteristics of Luciferase.....	11
1.2.2	Bio-analyses using Luciferase as a Reporter Gene.....	14
1.2.3	Split Luciferase Complementation and its Applications.....	15
1.3	Optogenetics for the Control of Biomolecules.....	19
1.3.1	The Subcellular Localizations of PIP3.....	20
1.3.2	Light Sensitive Proteins.....	21
1.3.3	Phytochrome B and Phytochrome Interaction Factor.....	21
1.3.4	Cryptochrome 2 and CIB1.....	23
1.3.5	Light Mediated CRY2-CIB1 Interaction.....	24
1.4	Aims of the Research in this Thesis.....	26
1.5	References.....	29
2.	Development of Bioluminescence Probes for the Analysis of PIP3 on the Cell Membrane.....	34
2.1	Introduction.....	34
2.2	Experimental Section.....	37
2.2.1	Materials.....	37
2.2.2	Construction of Plasmids for Mammalian Cell Expression.....	37
2.2.3	Cell Culture and Preparation of Stable Cell Line.....	38

2.2.4	Validation of the Production of PIP3 in CHO-PDGFR cell line.....	39
2.2.4.1	Immunostaining.....	39
2.2.4.2	Protein Translocation.....	40
2.2.5	Evaluation of the Bioluminescent Probes for PIP3 analysis.....	41
2.2.5.1	Immunoblot Analysis.....	41
2.2.5.2	Imaging of Probe Dynamics by Fluorescence Confocal Microscopy.....	42
2.2.5.3	Real-time Bioluminescence Assay for PIP3 in Live Cells.....	44
2.2.5.4	Bioluminescence Assays in Lysed Cells.....	45
2.2.5.5	Investigation of Probe Reversibility.....	47
2.2.6	Bioluminescence Assays of PIP3 Production.....	48
2.2.6.1	Comparison between Bioluminescence Intensities in Live Cell and Lysed Cell Assays.....	48
2.2.6.2	Quantitative Analyses for the Effects of PIP3 Agonist and Inhibitor.....	48
2.2.6.3	Time-dependent Bioluminescence Signals with the Lysis Buffer.....	49
2.2.7	Validation of a High-throughput Screening System.....	51
2.2.8	Visualization of PIP3 production by a Bioluminescence Microscopy.....	52
2.3	Results and Discussion.....	54
2.3.1	Schematics for the PIP3 Detection and Design of Fusion Proteins.....	54
2.3.2	Validation of the Production of PIP3 in CHO-PDGFR Cell Line.....	54
2.3.3	Characterization of the PIP3 Probes.....	55
2.3.4	Bioluminescence Analysis of PIP3 Production.....	56
2.3.5	Quantitative Analyses for PIP3 Activation and Inhibitory Effects of PIP3 Stimulants.....	59
2.3.6	Application to a HTS System.....	62
2.3.7	Imaging of PIP3 Production using a Bioluminescence Microscope.....	62
2.4	Discussion.....	66
2.5	Conclusion.....	68
2.6	Reference.....	69

3.	Optical Control of PIP3 Production on Cell Membranes...	71
3.1	Introduction.....	71
3.2	Experimental Section .....	74
3.2.1	Materials.....	74
3.2.2	Construction of Plasmids for Mammalian Cell Expression.....	75
3.2.3	Cell Culture.....	76
3.2.4	Viral Infection.....	76
3.2.5	Visualization of CRY2-CIBN Interactions on Cellular Compartments.....	77
3.2.5.1	Plasma Membrane.....	77
3.2.5.2	Endoplasmic Reticulum Membrane.....	78
3.2.5.3	Trans Golgi Network Membrane.....	78
3.2.5.4	Mitochondria Outer Membrane.....	78
3.2.6	Production of PIP3 by Blue Light Stimulation on the Plasma Membrane...	80
3.2.7	Reversibility of Light Regulated PIP3 Production.....	80
3.2.8	Induction of Directional Cell Movements by Optical Control of PIP3 Production on the Plasma Membrane.....	82
3.3	Results and Discussion.....	84
3.3.1	Schematics for the Optical Control of PIP3 Production and Design of Fusion Proteins.....	84
3.3.2	Localizations of the Fusion Proteins.....	85
3.3.3	Production of PIP3 by Blue Light Stimulation.....	86
3.3.4	Directional Cell Movements by Optical Control of PIP3 Production.....	87
3.4	Conclusion.....	88
3.5	References.....	89
4.	General Conclusion.....	90

# 1. General Introduction

## 1.1. Introduction of Phosphatidylinositol (3,4,5)-Trisphosphate (PIP3)

### 1.1.1. General Features of PIP3

Phosphatidylinositol 3,4,5- trisphosphate, derived from phosphatidylinositol (PI), is an amphiphilic molecule composed of a hydrophobic diacylglycerol (DAG) imbedded in a lipid double layer and a phosphorylated inositol head group facing toward the cytosol.<sup>1</sup> The head inositol ring of PIP3 consists of a single axial hydroxyl group at the D2 position and five equatorial hydroxyl substituents at the other positions. Among them the D3, D4, and D5 hydroxyl groups of the inositol ring are phosphorylated, resulting in a high negative charge of -7 exposed to the cytosol (Figure 1-1).<sup>2</sup>

PIP3 is a pivotal messenger involved in central cellular events, such as survival, embryonic development, motility, and vesicle transport. PIP3 is synthesized by class I phosphatidylinositide 3-kinase (PI 3-kinase), which is activated via receptor phosphorylation upon outside stimuli, to add one phosphate group at the 3' position of phosphatidylinositol 4,5- trisphosphate (PI(4,5)P2). In response to stimulation from growth factors, hormones, and chemoattractants, PIP3 is rapidly synthesized on the cell membrane and spatiotemporally recruits downstream molecules to a specific lipid membrane such as the inner leaflet of plasma membrane. Consequently, an array of response signals such as survival, cell movement, and embryonic development are triggered and regulated.<sup>3,4,5</sup> PIP3 is metabolized mainly by two lipid phosphatases that dephosphorylate PIs on the inositol ring: The PTEN (3'-phosphatase and tensin

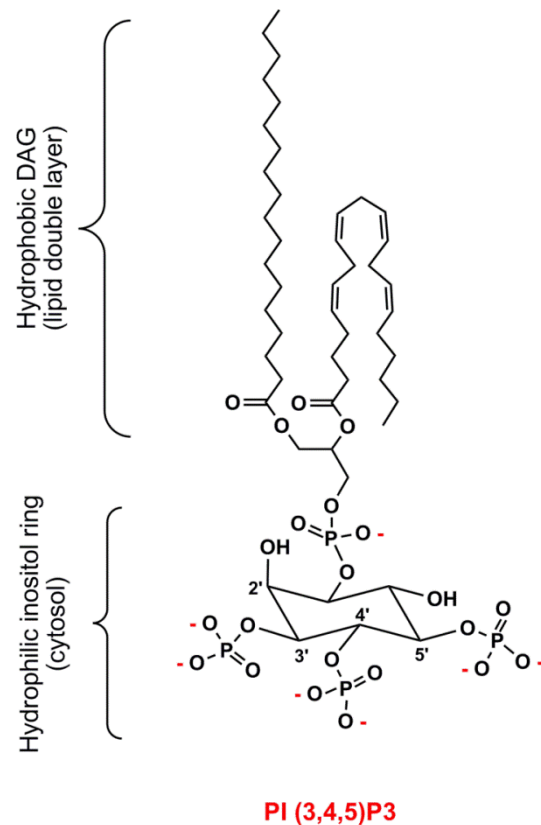


**Figure 1-1.** Molecular Structure of PIP3. PIP3 belongs to phosphatidylinositide (PI), of which the main structure is composed of a hydrophobic diacylglycerol (DAG) imbedded in a lipid double layer and a phosphorylated inositol head group facing toward the cytosol. The head inositol ring of PIP3 consists of a single axial hydroxyl group at the D2 position and five equatorial hydroxyl substituents at the other positions. The D3, D4, and D5 hydroxyl groups of the inositol ring are phosphorylated, resulting in a high negative charge of -7 exposed to the cytosol.

homolog) that removes the 3' phosphate group to form PI(4,5)P2, and the SHIP (Src homology 2 domain-containing inositol 5-phosphatase) that degrades the 5' phosphate group to produce PI(3,4)P2 (Figure 1-2). The metabolism of PIP3 or the inhibition of PIP3 synthesis also inhibits the PIP3 downstream effects.

PIP3 and its substrate PI(4,5)P2 comprise a small fraction of cell membranes, but they are responsible for the spatiotemporal regulation of many cellular processes.<sup>6</sup> Compared to PIP2, PIP3 is less abundant in the cell membrane even in elevated conditions. In un-stimulated cells, the PIP3 is normally present at approximately 0.1% of the amount of PIP2.<sup>7</sup> In contrast, PIP3 is elevated in an early embryo, growth factor stimulated cells, and polarized edge of chemotactic cells, with a sufficient level to trigger the downstream effects.<sup>3, 8, 9</sup>

The production and degradation of PIP3 at a controllable equilibrium are essential for maintaining the cell viability such as growth and development. On the contrary, overall elevated PIP3 level induces continuous activation of downstream molecules, which abnormally inhibit the signaling pathways for apoptosis and promote infinite cell growth. Such abnormal conditions are closely related to human cancers. For example, in many tumorigenic cells, an elevated PIP3 level is resulted from dysfunction of PTEN, which dephosphorylates PIP3. The abnormal PIP3 amount in various human cancer cells is also found to be caused by mutations of PI 3-kinase regulative subunit, which lead to a hyper activation of PIP3 synthesis. Although the PIP3 is known to be involved in fatal diseases such as cancers and diabetes, detailed mechanisms of its regulative roles are unclear because of limitations of current analytical methods. Spatiotemporal analysis of PIP3 production is, therefore, of vital importance to elucidate the biological functions and to clarify the PIP3 regulative roles to diseases.

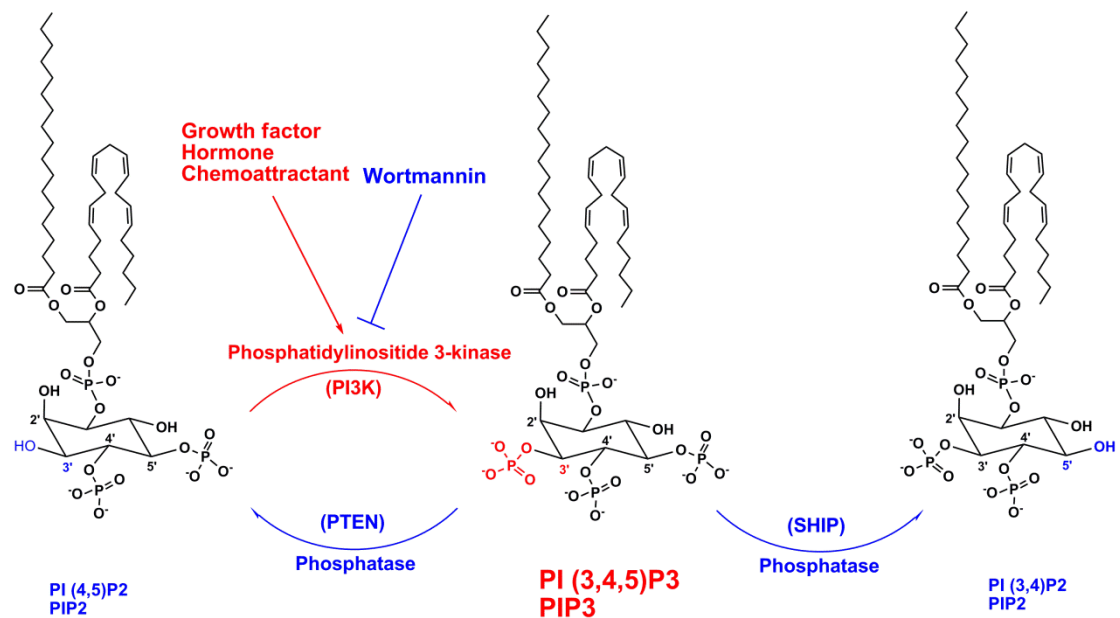


**Figure 1-2.** Major elements for the metabolism of PIP3. PIP3 is mainly synthesized from PI (4,5)P2, which is relatively abundant on the cell membrane, upon the stimulations of growth factors, hormones, and chemoattractants via the activation of phosphatidylinositol 3-kinase to add one phosphate group at 3'-position of the inositol ring. PI3K inhibitor such as wortmannin is able to inhibit the synthesis of PIP3. PIP3 is directly metabolized by phosphatases such as PTEN and SHIP, which remove a phosphate group from the 3'- and 5'- position of inositol ring respectively.

### 1.1.2. PIP3 Binding Modular Domains

PIP3 belongs to a class of phosphatidylinositols (PIs), which is composed of seven derivatives as signal molecules including three monophosphates, three bisphosphates, and one trisphosphate (PIP3), with net negative charges of -3, -5, and -7, respectively. These membrane signal molecules carry distinct messages to transduce to downstream pathways. In eukaryotic cells, many membrane-associative proteins, including a number of kinases involved in signal transduction pathways, have a preference to bind with one or more PIs. The binding between associative proteins and PIs is facilitated by a series of PI binding modular domains. These modular domains include pleckstrin homology (PH), FYVE (acronym of Fab1, YOTB, Vac1, and EEA1), phox homology (PX), and protein kinase C (PKC) homology (C2) domains, many of which are used to make recombinant proteins for PI studies.

Proteins that contain PIP3 binding modules can be recruited to interact with PIP3 after the PIP3 production on the cell membrane. The well-studied PIP3 binding module is Pleckstrin Homology domains (PHD/PH domain), which has been identified as one of the largest families of lipid-binding domains and has been intensively investigated. The PH domain is evolutionally conserved with a length of approximately 120 amino acids. It consists of one alpha helix and seven beta sheets connected with flexible loops (Figure 1-3A). Although various PH domains share little sequence similarity, the barrel of beta sheets creates a binding pocket with a similar conformation for the membrane-binding region. Electrostatic feature of the PH domains is a strong dipolar electrostatic potential, with a prominent positive lobe.<sup>10</sup> The electrostatic potential of phosphatidylinositols (PI) and phosphatidylserines (PS) on the lipid membrane helps to create a negatively charged environment of the plasma membrane, which attracts the positive lobe of the PH domain, thereby facilitating binding of the PH domain to membrane PIs.

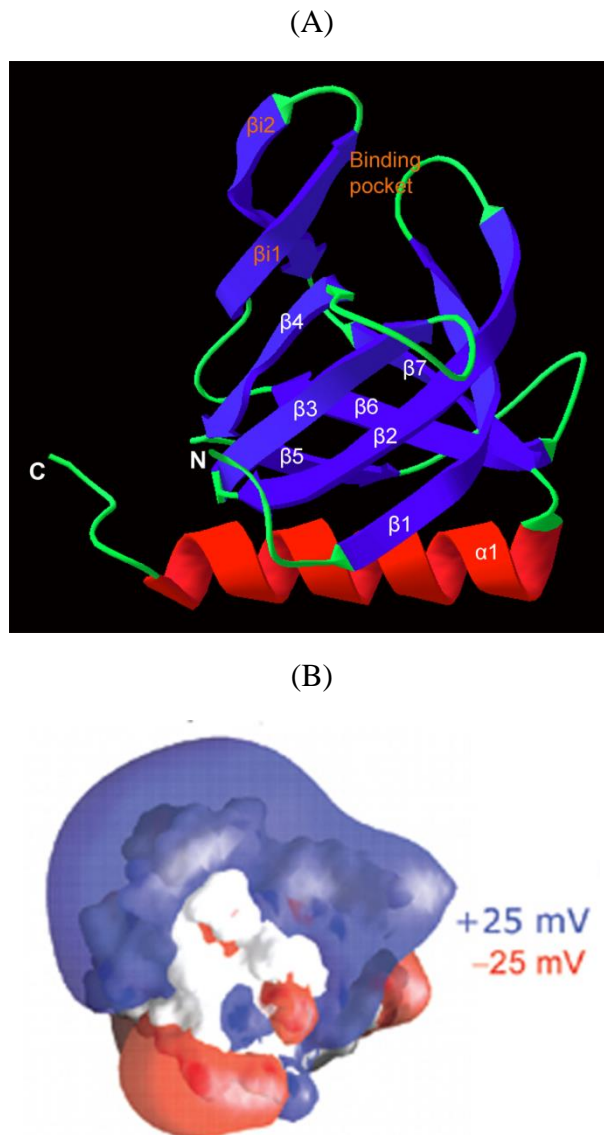


**Figure 1-3.** Structure of the GRP1 PH domain. (A) Conformation of GRP1 PH domain. It is composed of a nine-stranded anti-parallel  $\beta$  barrel capped by a C-terminal  $\alpha$  helix on one end of the barrel. The  $\beta_{i1}$  and  $\beta_{i2}$  indicate a hairpin insertion. The  $\beta_{i1}/\beta_{i2}$  loop, together with  $\beta_1/\beta_2$  loop and  $\beta_3/\beta_4$  loop, generates a specific PIP3 binding pocket.<sup>11</sup> (B) Model for electrostatic potential of the GRP1 PH domain. A strong dipolar electrostatic potential exists and contours at +25 mV and -25 mV. The molecular surface and electrostatic potential are calculated with GRASP (Graphical Representation and Analysis of Surface Properties). Reprinted from ref 10. Copyright 2003 DiNitto et al.

In order to selectively recognize PIP3 in living cells, a PH domain needs to exhibit

an affinity for PIP3 at least one to two orders of magnitude higher than that for PIP2, because even in stimulated cells, the amount of PIP2 is much higher than that of PIP3.<sup>12</sup> In a survey of PH domains, however, most PH domains were found to bind PIP3 with low selectivity because of the similarity between different PIs. A PH domain of general receptor for phosphoinositides 1 (GRP1) has been identified as a PIP3 binding modular domain with high affinity and selectivity.<sup>13</sup> It possesses a high electrostatic potential contours at +25 mV and -25 mV (Figure 1-3B), which contributes to the translocation from the cytosol to the lipid membrane and the binding with PIP3. It exhibits a 650-fold higher specificity to PIP3 than it does to PIP2.<sup>14</sup> Therefore, the PH domain of GRP1 is ideal for PIP3 recognition in living cells.

### 1.1.3. Analytical Methods for PIP3

In order to reveal the complex roles of PIP3 in signaling pathways and its relationships with human diseases, extensive PIP3 analyses have been performed. Initially, biochemical method to measure the total cellular level of PIP3 has been developed. This method involves the use of PIP3-specific antibodies for the analysis of total PIP3 amount in stimulated cells.<sup>15</sup> For the purpose of elevating the PIP3 synthesis to a detectable PIP3 level, living cells are stimulated with PIP3 agonist before fixing and blotting the cells with a PIP3 antibody. This method is strongly dependent on the quality of the PIP3-specific antibody. Furthermore, the fixation procedure as well as the membrane permeabilization step using a surfactant destroys the original electrostatic property of the cell membrane. The concomitant washing steps are also likely to relocate membrane molecules. As a result, the PIP3 signals are visualized as clusters inside cells distant from the plasma membrane. A surrogate assay is to evaluate PIP3 level indirectly by examining the phosphorylation level of PIP3 downstream proteins, such as the protein kinase B (PKB).<sup>16</sup> However, the PKB phosphorylation is possibly

disconnected from PIP3 level, because the PKB does not only respond to PIP3 but is also recruited to PIP2. The lack of specificity leads to an inaccurate evaluation of the PIP3 level.<sup>11</sup>

For an accurate evaluation of absolute PIP3 level, instrumental analyses such as capillary zone electrophoresis, high-performance liquid chromatography, and thin layer chromatography, coupled with isotope tags or mass spectrometry, are used to analyze cellular PIP3.<sup>17,18</sup> For example, Jonathan Clark et al. introduced a PIP3 quantification methodology based on mild PIP3 phosphate methylation coupled with HPLC-MS to analyze the cellular PIP3. The specific methylation of PIP3 discriminates PIP3 signals with those of other fatty-acyl species. This method enables evaluation of multiple fatty-acyl species of PIP3 in unstimulated mouse/human cells or tissues, as well as enables the identification of PIP3 increases upon PIP3 agonist.<sup>17</sup> Although the instrumental quantification facilitated analyses of PIP3 amounts with high selectivity, the in-vitro methods involve cell-demolishing membrane lipid extraction, during which the sample pretreatment partially decomposes the PIP3. Furthermore, the accurate subcellular localizations of PIP3 couldn't be addressed by these in vitro methods.

To overcome the limitations caused by sample pretreatment, methods of live cell fluorescence imaging have been developed in order to visualize the PIP3 dynamics. Taking advantage of the PH domain of GRP1 that specificity binds PIP3, optical probes enable the analysis of dynamic changes in a cellular PIP3 amount in real time. For example, PH domain is genetically fused with an enhanced green fluorescent protein (EGFP) for the PIP3 detection (Figure 1-4 (A)). After the PIP3 is produced on the plasma membrane upon ligand stimulation, the fusion proteins translocate from cytosol to the plasma membrane by the PIP3-PH domain interactions and therefore indicate PIP3 production.<sup>19</sup> In addition, a fluorescence resonance energy transfer (FRET) probe was designed for PIP3 analysis, where the FRET ratio changes indicate the amount of

PIP3 produced on the cell membrane over time. By examining the FRET ratio, Moritoshi Sato et al. demonstrated that the production of PIP3 on the endoplasmic reticulum and Golgi apparatus was triggered by receptor endocytosis (Figure 1-4 (B)).<sup>20</sup> These fluorescent probes are attractive in real-time analysis of PIP3 in living cells; however, the observation area that can be viewed under a fluorescence confocal microscope is limited. Also, the toxicity introduced by the excitation light induces reactive oxygen species (ROS) that cause cell damage, and moreover, the photo-bleaching property of a fluorescent protein causes fluorescence fluctuation, which makes it inadequate for long-term observations. Therefore, the fluorescence probes are unable to perform quantitative and temporal analyses of PIP3. New method for PIP3 analysis is needed for further PIP3 study, which facilitates potential applications related to PIP3 such as the identification of potent PIP3 agonists and inhibitors for drug screening.

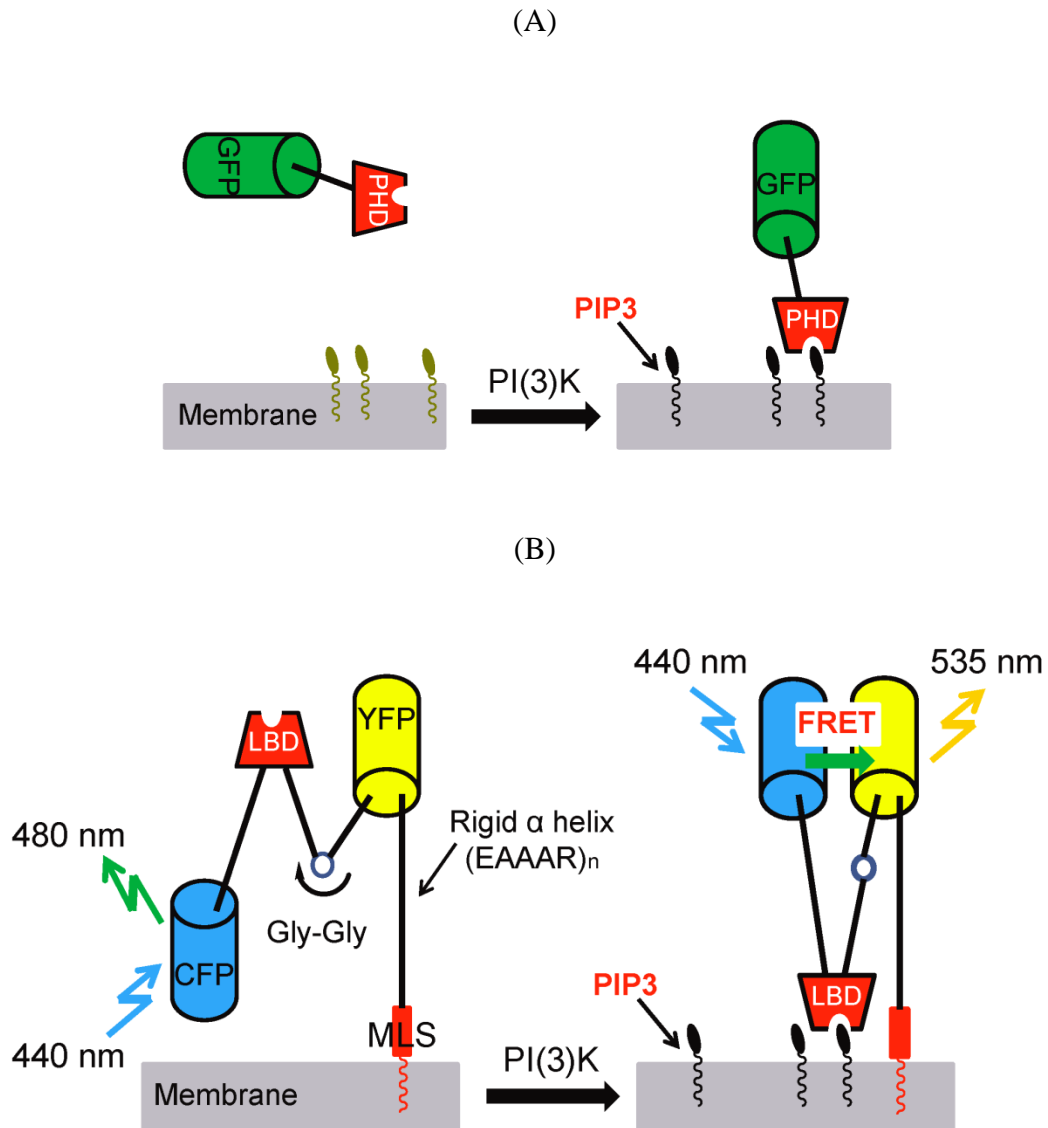


**Figure 1-4.** Probes for the PIP3 analysis. (A) A fluorescent probe for PIP3 detection. A green fluorescent protein is fused with a PH domain expressed in the cytosol. The translocation of the fusion protein indicates the PIP3 production. (B) A FRET probe for the analysis of PIP3. CFP and YFP are mutants of GFP, and processes desirable fluorescence spectrum for the FRET phenomena. After a PIP3 is produced on a cell membrane, a lipid binding domain (LBD) binds to the PIP3 to initiate a flip-flop-type conformational change, which facilitates the efficiency of FRET from CFP to YFP.

## 1.2. Introduction of Bioluminescence Analysis

Bioluminescence, which was first studied by the French pharmacologist Raphaël Dubois, has been utilized as an analytical tool to modern scientific research.<sup>21</sup> Bioluminescence is the production and emission of cold light by a luminous organism for purposes such as communication. It exists in a range of species such as marine animals, bacteria, fungi, algae, and insects. Bioluminescence, which functions in living organisms to convey various signals, is produced by a luciferase enzyme catalyzing a luciferase substrate to react with oxygen, sometimes with cofactors such as calcium ions or ATP. Bioluminescence provides marked benefits over fluorescence in the analysis of biological events, the main one being its non-invasiveness to the physiological environment because it obviates the use of excitation light and enables longitudinal observations.<sup>22</sup> The absence of excitation light greatly reduces background interference in chemical library screening and eliminates interference with auto-fluorescent compositions of living tissues. Furthermore, the larger dynamic range of bioluminescence compared with fluorescence is beneficial for quantitative studies, especially for screening.<sup>23,24</sup>

### 1.2.1. Characteristics of Luciferase

Luciferase is a class of oxidative enzymes that catalyze a bioluminescent reaction to produce light. Organisms regulate their light production using a variety of luciferases and substrates in light-emitting reactions. The generation of light by a luciferase is a multistep process. Commonly, a substrate is oxidized to electronically excited peroxide with high-energy chemical bonds. Then, the oxidized substrate transforms from an excited state with high energy to a ground one, during which excessive chemical energy is efficiently transferred into light (Figure 1-5). Among the diverse bioluminescence systems, marine luciferases use coelenterazine as a substrate, whereas insect luciferases

use D-luciferin (benzothiazole). The bioluminescence system using insect luciferase and D-luciferin is an optimum pair to produce low background and highly quantitative bioluminescence signals. The D-luciferin is a highly stable luciferase substrate and it permeates easily into cells or tissues. This feature makes insect luciferases beneficial for non-invasive analyses of biological events.<sup>25</sup>

Firefly luciferase is a well-known insect luciferase derived from firefly *Photinus pyralis* ( $\lambda_{\text{max}} = 552 \text{ nm}$ ), of which the structure and characteristics have been extensively studied.<sup>26</sup> Firefly luciferase consists of an N-terminal domain and a C-terminal domain connected by a flexible hinge, which creates an active site between the two domains.<sup>27</sup> The luciferase undergoes a conformational change, such that the N- and C- domains come together to exclude water molecules for prevention of the ATP hydrolyzation or to exclude the electronically excited peroxide, to enclose a substrate.<sup>27</sup> Through widely used for reporter proteins, firefly luciferase has a feature of pH sensitivity, that the luciferase activity reaches optimum level only at pH 7.8. Also, the light produced by firefly luciferase is largely absorbed by hemoglobin, which is a light absorber widely exists in tissues. The pH dependence and the firefly luciferase spectrum, which is close to the tissue auto-fluorescence, hinder its applications. To circumvent these drawbacks, efforts have been made to obtain luciferases with a desirable spectrum, an enhanced brightness and structural stability. For instance, a pH insensitive enhanced beetle luciferase (Eluc) from the Brazilian click beetle *Pyrearinus termitilluminans*, which emits green light ( $\lambda_{\text{max}} = 538 \text{ nm}$ ) and produces over 10 fold stronger light compared to firefly luciferase, was developed by Yoshihiro Ohmiya, et al.<sup>25</sup> Another example is a red-emitting luciferase named Ppy RE-TS ( $\lambda_{\text{max}} = 610 \text{ nm}$ ), which is mutated from the *Pyrearinus termitilluminans* luciferase, engineered by Branchini, Bruce R. et al.<sup>28</sup> The red-emitting luciferase produces bioluminescence signals able to penetrate tissues for the bioluminescence

tissue imaging.

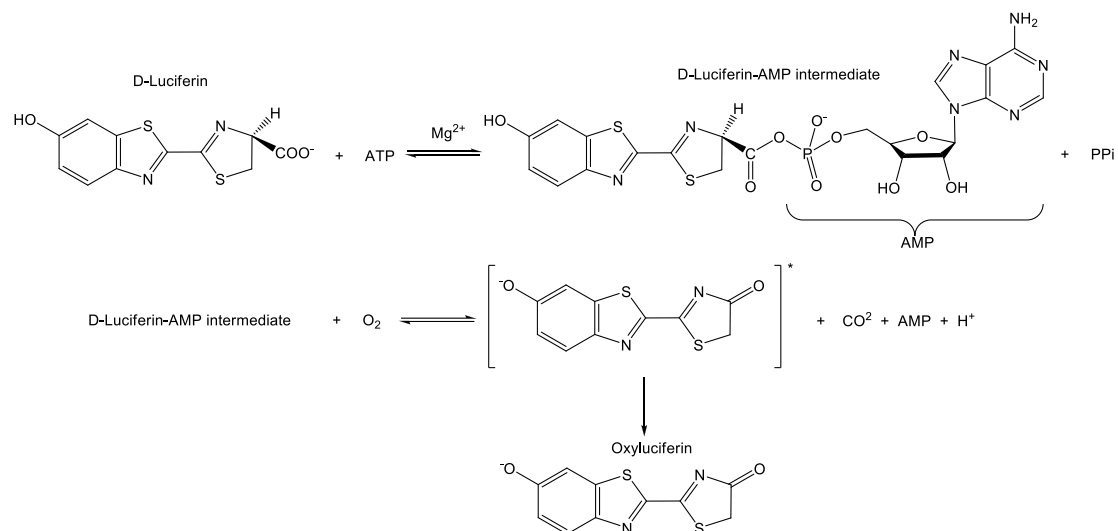


**Figure 1-5.** The bioluminescence reaction catalyzed by a beetle luciferase. The production of bioluminescence is composed of two steps: Firstly, intermediates of luciferyl-AMP are formed with the assistances of ATP and Mg<sup>2+</sup>; secondly, oxidation of the intermediate produces excited oxyluciferin with high-energy chemical bonds. When the excited state oxyluciferin returns to its ground state, the excessive energy is efficiently transferred into light.

### 1.2.2. Bio-analyses using Luciferase as a Reporter Gene

Whereas the fluorescence technique that use fluorescent proteins (e.g., green fluorescent protein (GFP) and its derivatives) as probes has greatly contributed to the progress of cell biological research, bioluminescence technique has emerged as a new approach for analyzing cellular events. Bioluminescence system has enabled broad applications due to its high sensitivity, ease of use, and cost effectiveness. It was widely used as an optical reporter system to study biological processes in living cells and organisms because of a low background in mammalian cells.<sup>29</sup> Briefly, a Luciferase gene is incorporated genetically into various hosts to monitor biological events such as a gene expression or production of a biomolecule, and also to visualize a specific cell type.<sup>25</sup>

Bioluminescence has been exploited as a powerful analytical tool for cellular studies. The luciferase gene was first used as a reporter for monitoring promoter activities. The observation of the transcriptional activity of a promoter is facilitated by insertion of the promoter into a plasmid that contains cDNA of a luciferase and by monitoring the luciferase activities over time.<sup>30, 31</sup> A typical example is the study of circadian rhythm. A luciferase is fused with Per2 or HSE promoters to visualize a synchronization of circadian rhythms of populated cells upon oxidative stress or heat shock.<sup>32,33</sup> Another application is the analysis of a biomolecule production using a bioluminescence indicator. For example, the firefly luciferase activity is strongly dependent on the concentration of ATP when concentrations of other components for the luciferase system are relatively stable. A calcium sensitive probe using luciferase has been developed to monitor calcium quantities inside cells.<sup>34</sup>

Another attractive application of the bioluminescence system is the bioluminescence imaging (BLI), which has become a widely used optical technology for interrogating and analyzing molecular features inside cells or in model animals.

Other than the quantitative measurements of bioluminescence signals, a target of a luciferase assay in living cells can be visualized under a microscopy with relevant spatial and temporal resolution. The strong advantage of a bioluminescence system is that it causes minimum cell damage because the bioluminescence reaction requires no excitation light. Therefore, the visualization of biomolecules inside a cell using bioluminescence enables a straightforward and reliable understanding of molecular mechanisms. In the researches of medical field, luciferase has been engineered to label cancer cells, immune cells, etc. and the noninvasive longitudinal imaging of living organisms is performed to observe circulation of target cells in small animals.<sup>35</sup>

### 1.2.3. Split Luciferase Complementation and its Applications

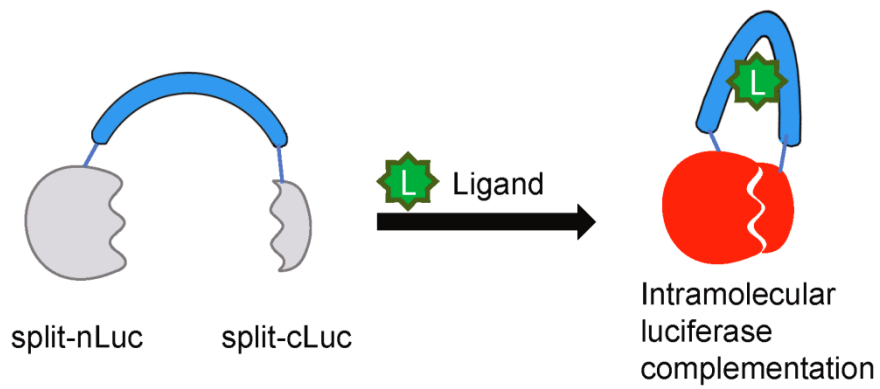
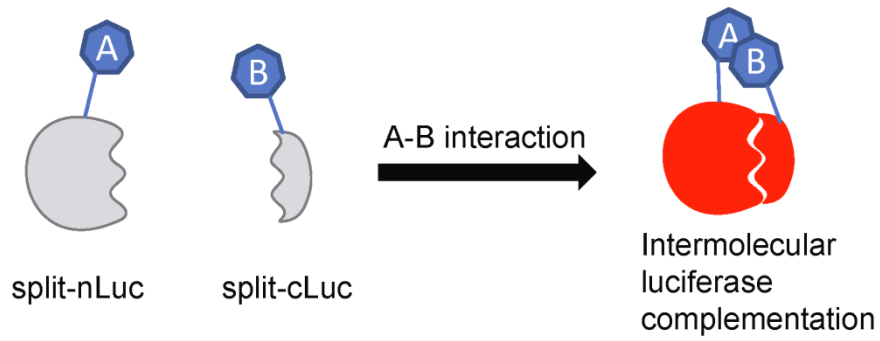
Conventionally, a full-length luciferase is genetically incorporated and expressed in cells to identify a specific cell type or to visualize a biological event in a non-luminescent host. However, such analyses are insufficient to interrogate molecular and biological functions spatiotemporally inside cells. In order to apply the bioluminescence technology further for the non-invasive analysis of biomolecules, a split-luciferase complementation strategy has been described.<sup>36</sup> For the establishment of the split-luciferase complementation system, a full-length luciferase is dissected to an N-terminal fragment and a C-terminal fragment. Consequently, the enzymatic activity is lost completely. When the fragments are brought into mutual proximity, the complementation of luciferase fragments is initiated. Then the structure of an active luciferase is reconstituted, and the reconstitution causes the production of bioluminescence signals.<sup>36</sup>

The split luciferase complementation probes have been designed as versatile bioluminescence indicators to non-invasively visualize cellular events such as protein-protein interaction, protein conformation change, protein translocation, and protein

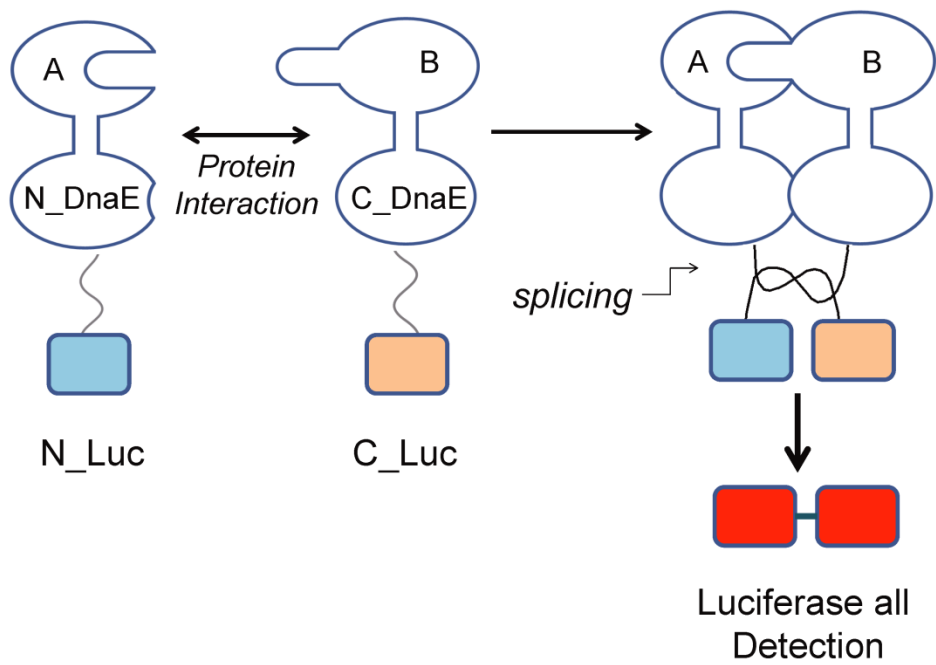
phosphorylation by either intermolecular or intramolecular fragment complementation (Figure 1-6).<sup>37</sup> In the intermolecular design, genes of split N- and C- luciferase fragments are respectively fused to genes of two separate proteins. Such design analyzes interactions and dynamics of two proteins in living cells (Figure 1-6B).<sup>36</sup> An interaction on the plasma membrane between GRCRs (G-protein coupled receptors) with  $\beta$ -arrestin has also been examined by a pair of split luciferase probes (Figure 1-6C).<sup>38</sup> Furthermore, split luciferase probes are used for protein translocation studies such as a study of nuclear transport.<sup>39</sup> On the other hand, intramolecular design has incorporated both N- and C- terminal luciferase fragments within one fusion protein to analyze a protein conformational change. The target protein is fused in the middle of the construct and undergoes a conformation change to bring the N- and C- terminal luciferase fragments into closer proximity to initiate the luciferase complementation. This design is applicable for the analysis of protein phosphorylation (Figure 1-6D),<sup>40</sup> which is usually accompanied by a protein conformational change. Additionally, split luciferase complementation strategy has succeeded in other spatiotemporal studies of pH,<sup>41</sup> cAMP, and cGMP.<sup>42,43</sup>

The split and reconstitution of a luciferase involve deactivation and recovery of a luciferase activity. The specific site to dissect an active luciferase and the complementation features of luciferase fragments are of crucial importance. Efforts have been made to investigate the complementation between split luciferase fragments from different dissection sites or different luciferases. Basically, the bioluminescence recovery is examined by fusing genes of different luciferase fragments respectively with genes of FKBP and FRB, and by determining the interactions between the corresponding proteins. FKBP and FRB form a complex structure in the presence of rapamycin. The complementation efficiency of luciferase fragments is obtained by monitoring bioluminescence recoveries upon the rapamycin

(A)



(B)



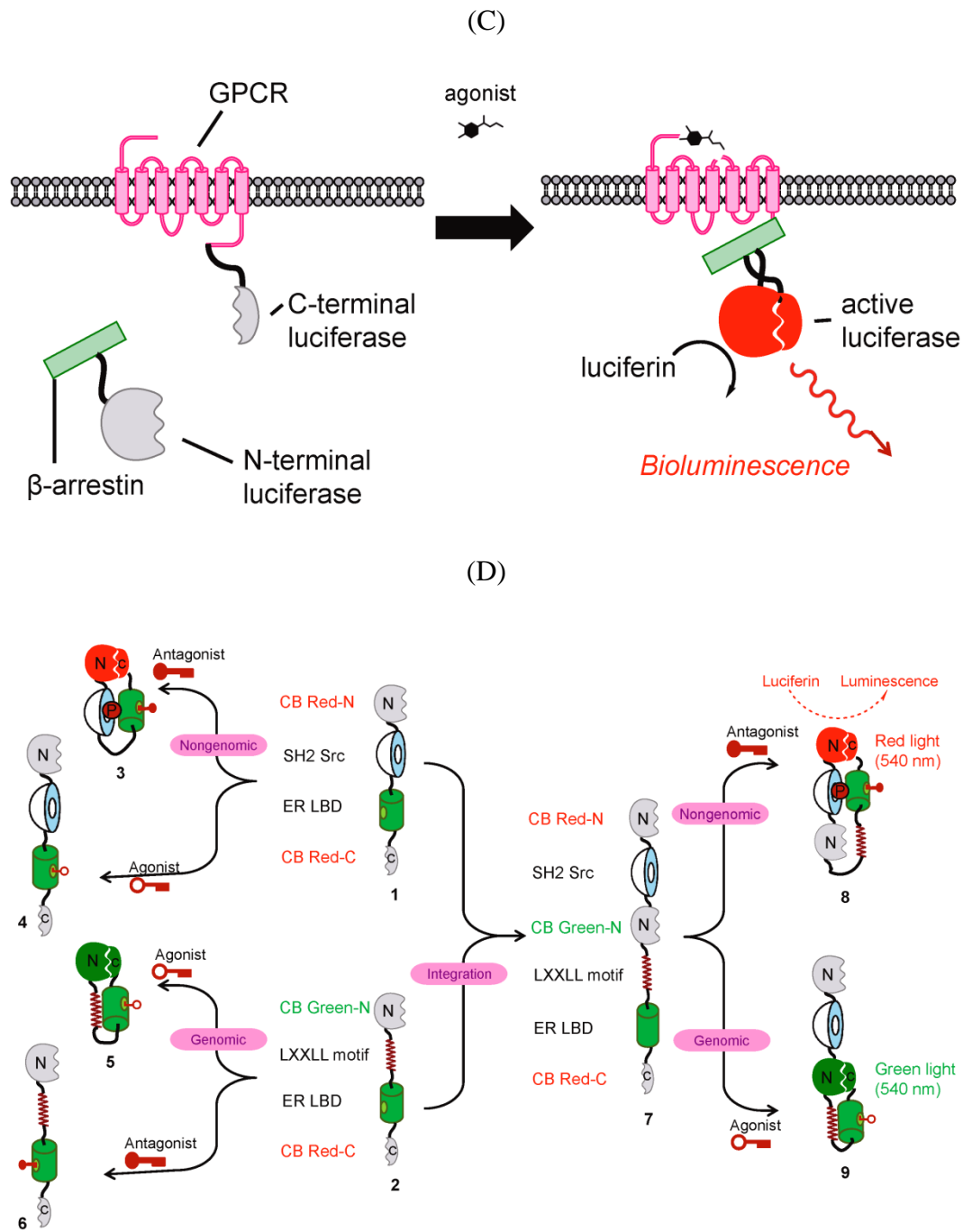


**Figure 1-6.** Split luciferase complementation probes for the analyses of cellular biological events. (A) The classification of split luciferase probes. Intermolecular complementation is adopted in studies of protein-protein interactions and protein translocation, whereas intramolecular complementation is utilized in the analyses of protein conformational changes and protein phosphorylation, etc. Probes are designed for: (B) The bioluminescence analysis of protein-protein interactions. (C) Visualization of ligand-receptor interaction in living cells. (D) Quantitative analysis of protein phosphorylation.

stimulation.<sup>44</sup> Split luciferase probes with desirable features are also rationally designed and obtained by optimizing the dissection site of a luciferase gene. For example, an McLuc1 (multiple-complement luciferase fragment) has been developed from screening of randomly mutated C-terminal fragments of Click beetle red luciferase (CBR) by Hida et al.<sup>44</sup> Mcluc1 has shown remarkable capabilities to complement with N-terminal fragments of different luciferases. The combination of Mcluc1 as a C-terminal luciferase fragment and CBRN (1-415 amino acid of Click Beetle Red luciferase) as an N-terminal fragment has a relatively high affinity and their interaction is reversible. The maximum emission wavelength of the reconstituted luciferase is 613 nm, which is desirable for tissue penetration. The features of McLuc1 and CBRN make the pair of luciferase fragments applicable to establish a PIP3 probe for the analysis of its production by bioluminescence.

### 1.3. Optogenetics for the Control of Biomolecules

The basis of life consists of bio-molecular behaviors that occurred with diverse spatial precisions and manners inside cells. Current analytical chemistry studies are not confined with analyzing the amount and dynamics of a chemical or a biomolecule, but are engaging in establishing novel platforms to precisely control a well-defined biological event to analyze relevant molecular functions. The term “Optogenetics” was first defined in 2006, when light was used to control specific populations of neurons, in which light sensitive proteins are expressed, without affecting other neurons in the brain at high spatiotemporal resolution.<sup>45</sup> It combines optics and genetic engineering to either stimulate or inhibit cellular activity via light sensitive proteins. Nowadays optogenetic methods are also widely used as a tool to tamper a range of biological events such as protein-protein interactions,<sup>46,47,48</sup> motility study of living cells,<sup>49</sup> and control of signal transduction pathways.<sup>50,51</sup>

### 1.3.1. The Subcellular Localizations of PIP3

Although PIP3 is known to be tethered in the lipid double layer which is the basic structure of all cell membranes, most previous studies of PIP3 disregarded the PIP3 production on distinct cell membranes. The main reason of this ignorance is that the production of PIP3 is always triggered by stimulations such as growth factors, hormones and chemoattractants outside the cells.<sup>19,52,53</sup> Upon ligand activation, the receptors on the plasma membrane receive signals and rapidly recruit PI 3-kinase to initiate the PIP3 production in situ, which is generally visualized by the translocation of PIP3-binding PH domains from the cytosol to the plasma membrane.<sup>19,50,54</sup>

The PIP3 production on either plasma membrane or endomembranes (Endoplasmic reticulum and Golgi apparatus) has been analyzed by a fluorescence resonance energy transfer (FRET) probe.<sup>20</sup> The probe proved that the PIP3 level on the endomembrane is elevated by receptor endocytosis from the plasma membrane after its production. Although this result demonstrates that PIP3 exists on the endomembranes, the functions of PIP3 on separate organelle membranes are still obscure because the production of PIP3 on the endomembranes is passively induced by chemical stimulations that lack the spatiotemporal regularity. The investigation of PIP3 on places other than the plasma membrane remains scarce due to the lack of analytical methods to monitor the PIP3 production.

The composition of biological membranes is highly complex and variable, depending both on the type of cell and the organelle of interest. Lipid composition also varies within organelles. Although sometimes cell membranes are interchangeable, the PIP3 molecules may naturally exist in subcellular membranes such as an organelle membrane, building up networks to spatiotemporally mediate downstream effects. In substitution of chemical stimulation to produce PIP3 with poor spatial regularity, a

method to selectively perturb the produce PIP3 on distinct destination of cell membrane is in need.

### 1.3.2. Light Sensitive Proteins

In order to circumvent the drawbacks of chemical stimulation for PIP3 production, optogenetics emerged as an effective tool to manipulate subcellular production of PIP3. The core of an optogenetic system is the light sensitive protein that responds to light stimulation and enables the delivery of light signal to precise intracellular locations. Optogenetic technology has been widely used in the field of neuronal science to control neuron circuits. Previously, channelrhodopsin and halorhodopsin/ archaerhodopsins have been reported to be capable of turning neurons on and off when neuron cells expressing these proteins were exposed to different wavelengths of light.<sup>55,56,57</sup> Channelrhodopsin and halorhodopsin/ archaerhodopsins are light-sensitive ion-channel proteins which initiate the ion flow through neuron cell membranes upon light stimulation. These are extremely useful tools to perturb neuron circuits because the light induced events are extremely fast, reversible, and also considerably safe.<sup>58</sup>

Although the light sensitive proteins in optogenetics have gained notices from neuroscience, the optogenetic technique has opened a broader path for the analysis and control of biological events in living cells or organisms. The light controllable protein-protein interactions, in particular, have enabled intelligent design to the spatiotemporal control of biological functions.

### 1.3.3. Phytochrome B and Phytochrome Interaction Factor

Phytochrome B (Phy) and Phytochrome Interaction Factor (PIF) modules are two interactive proteins that can be genetically expressed in target cells for the light mediated regulation of diverse biological processes.<sup>59,60,61</sup> Phytochromes are a class of

photoreceptive signaling proteins that mediate light-sensitive processes in plant by detecting red and near-infrared light. In *Arabidopsis thaliana* cells, Phytochrome B undergoes photoisomerization after covalently binds with a tetrapyrrole chromophore phytylcyanobilin (PCB). Upon red or far red light irradiation, the Phy-PCB complex changes its conformation to a Pr (red-absorbing) state or a Pfr (far-red-absorbing) state. PIF only binds the red absorbing form of phytochrome complex (Phy-PCB) (Figure 1-7).<sup>47</sup> The interaction between Phy and PCB is rapid, reversible and the degree of interaction is correlated with light intensity.<sup>51</sup>

The Phy-PIF optogenetic system can be designed as a light inducible signal imputer with high spatial accuracy inside cells. It is widely used for the perturbation of protein translocation because the system is able to produce both “on” and “off” signals in millisecond timescale. A light-inducible targeting system in budding yeast has been established using the optical controlled Phy-PIF interactions to target proteins to intracellular organelles.<sup>51</sup> An inelible drawback of the Phy-PIF system, however, is the requirement of concentrated exogenous chromophore of tetrapyrrole chromophore (eg. 50  $\mu$ M PCB), which needs to be laboriously purified.

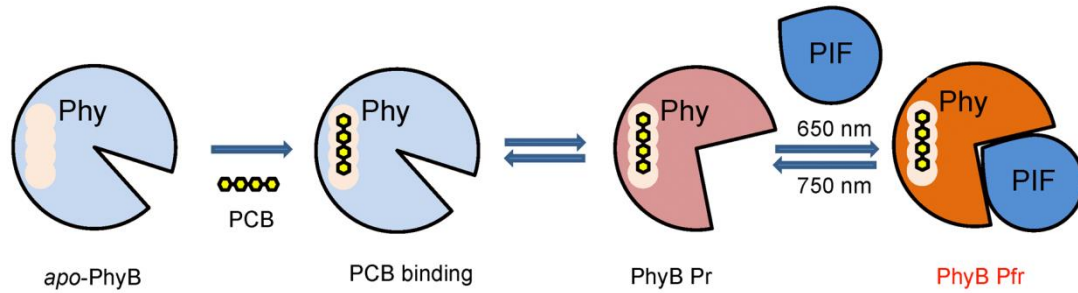


**Figure 1-7.** Schematic of the Phytochrome B-PIF interaction. A chromophores PCB (phycocyanobilin) covalently binds with *Arabidopsis thaliana* *apo*-PhyB. Upon 650 nm light irradiation, the PCB binding PhyB undergoes a conformational change from a Pr (red-absorbing) state to a Pfr (far-red-absorbing) state. When irradiated with 750 nm light, the PhyB-PCB complex returns to the Pr state. PIF only binds the red absorbing form of Phy-PCB complex.

#### 1.3.4. Cryptochrome 2 and CIB1

Cryptochromes are photolyase-like blue-light receptor proteins that mediate photomorphogenic development in plants and regulate light responses such as circadian clock in plants and animals.<sup>62,63,64</sup> Cryptochrome 2 (CRY2) of the *Arabidopsis thaliana* has drawn attention after the identification of CRY2-CIB1 interaction upon blue light stimulation ( $\lambda < 500$  nm). CIB1 is a cryptochrome-interacting bHLH (basic helix-loop-helix) protein. It is a nuclear protein that colocalizes with CRY2 in the nucleus. Compared to CRY2, whose biological role is relatively controversial, CIB1 receives informations from CRY2 and promotes downstream effects by interacting with CRY2 and then regulates transcription in plant cells.<sup>65</sup>

#### 1.3.5. Light Mediated CRY2-CIB1 Interaction

CRY2 has absorption peaks at 360 nm and 450 nm (blue-light area) and interacts with CIB1 (Figure 1-8(A)). The interaction is blue-light specific for both full-length CIB1 and N-terminal domain of CIB1 (CIBN).<sup>65</sup> When irradiated with red light or kept in darkness, the pair of CRY2-CIB1/CIBN would initiate the dissociation. The mechanisms of CRY2-CIB1 interaction, however, have not yet been completely resolved. After blue light irradiation, CRY2 changes into a photo-excited state, and binds with CIB1. This interaction is dependent on both blue light and Flavin/pterin chromophores. It is proposed that the photoexcitation of CRY2 is mediated by a chromophore flavin adenine dinucleotide (FAD), which absorbs blue light and was found non-covalently associated with CRY2. On the other hand, the fully reduced FADH<sub>2</sub> absorbs little visible light. The reduction of FAD is shown in Figure 1-8(A), which is believed to be leading to the conformational change of CRY2.<sup>66</sup>

A truncated version of CRY2, the conserved N-terminal photolyase homology region (PHR), that binds flavin and pterin chromophores, can also interact with CIB1/CIBN. This reaction is fast (sub-second time scale) and reversible. The advantage of the CRY2-CIB1 interaction over the PHY-PIF interaction in optogenetic system is the co-factor of chromophores. CRY2-CIB1 uses endogenous co-factors that commonly existed in many cell lines. In addition, the interaction of CRY2-CIB1 can be activated by two-photon microscopy, allowing potential use in whole organisms.

Genetic engineering of CRY2-CIBN enables to control various cellular signaling with blue light. This module of optical control is useful for controlling a broad range of biological phenomena. The production of PIP<sub>3</sub> on distinct organelle membranes can be designed by attaching one of the CRY2-CIBN proteins to a subcellular membrane and modifying the other one with protein modules that are sufficient to produce the PIP<sub>3</sub>.

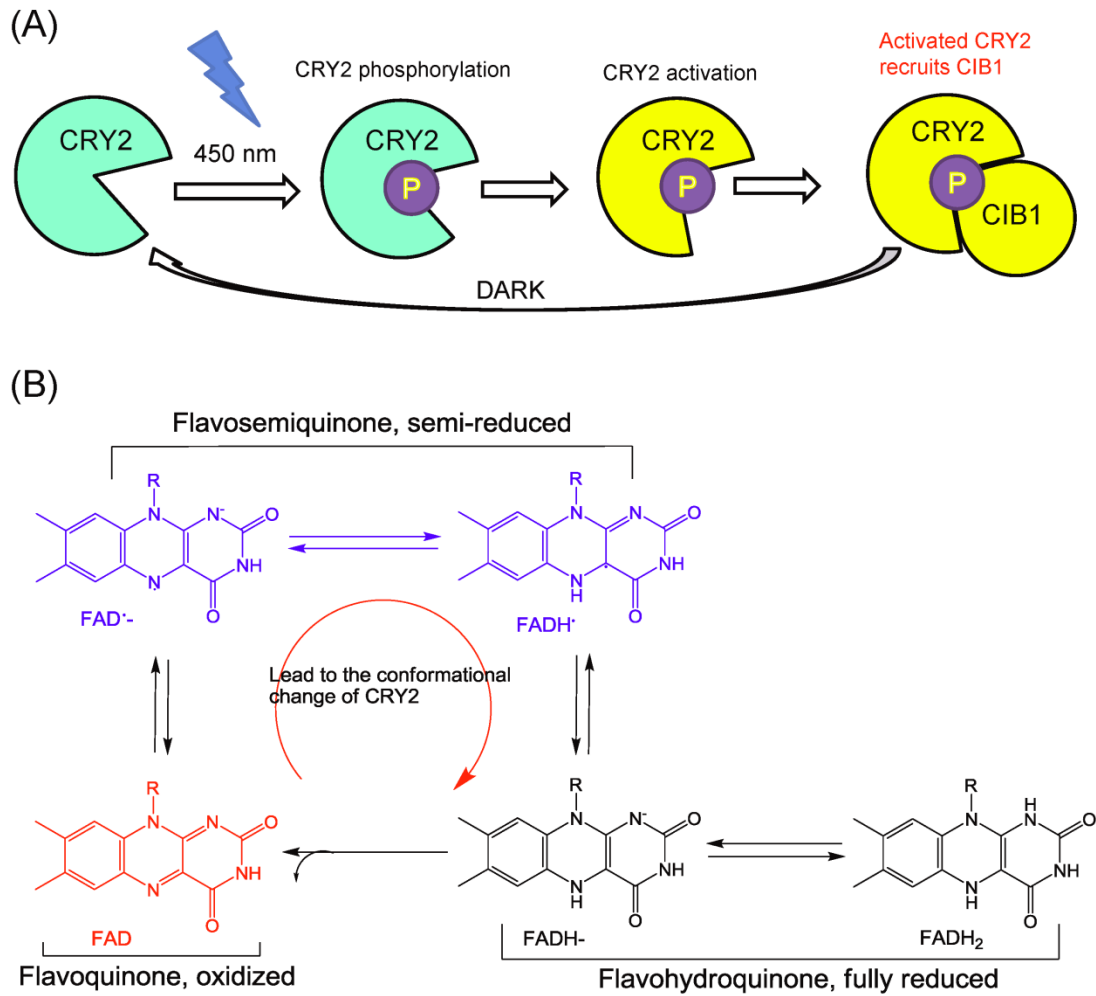


**Figure 1-8.** Schematic of the Cryptochrome 2-CIB1 interaction. (A) Light-gated activation of CRY2-CIB1 interaction. The CRY2 undergoes activation upon blue light irradiation by the light dependent phosphorylation. The activated CRY2 recruits CIB1 in subsecond timescale. When returning to the dark environment, the CRY2 returns to its original state and dissociate the CIB1. (B) Reduction circle of the CRY2 chromophores: Flavin Adenine Dinucleotide (FAD). The oxidized form, semi-reduced form, and the fully reduced form of FAD are shown. Oxidized FAD effectively absorbs blue light, whereas the fully reduced FADH<sub>2</sub> absorbs little visible wavelengths of light. R abbreviates for the adenine dinucleotide.

## 1.4. Aims of the Research in this Thesis

As is described in the previous section, the existing PIP3 analysis is based on in vitro biochemical assays and instrumental analysis. However, in vitro assays have drawbacks of cell-demolishing pretreatment that produces plausible quantification of PIP3. In vivo probes using a fluorescent protein have been developed to visualize the PIP3 production in single cell using Pleckstrin Homology domain of GRP1, which specifically and efficiently binds PIP3 after its production. Fluorescent probes have enabled effective PIP3 visualization in living cells; however, limitations exist in terms of the fluorescence observation, of which intrinsic fluorescence photobleaching/blinking and the complicated equipment confine further applications.

Bioluminescence has been evolved as a desirable tool over fluorescence for the non-invasive analyses of biological events with wide applicability because of its low background, its ease of use and the cost effectiveness. Split luciferase complementation has enabled spatiotemporal studies that are usually difficult when using a full-length luciferase. An active luciferase was dissected into two inactive fragments and fused respectively with two proteins. The spatial regulation is realized by predominantly targeting one protein at a specific area of a cell. When the target protein interacts with each other on the designated region, the luciferase fragments reach close proximity to reconstitute into an active luciferase and recover the bioluminescence signal. Split luciferase complementation is an effective way to evaluate the degree of protein-protein interactions by recovered bioluminescence signals.

Therefore, split luciferase complementation is suitable for the analysis of PIP3 on the cell membrane. Because PIP3 is largely produced on the plasma membrane to mediate subsequent functions upon ligand stimulations, in chapter 2, we focused on the development of bioluminescent probes to assess the PIP3 production on the plasma membrane by quantified bioluminescence signals. For this purpose, we designed split

luciferase probes including PH domain of GRP1, the PIP3 binding motif, to spatiotemporally analyze the production of PIP3 upon ligand stimulation. The scheme of probe design is as follows: the split N-terminal luciferase fragment is predominantly expressed on the plasma membrane by fusing with a PM targeting sequence, whereas the C-terminal luciferase fragment is fused with tandem PH domains expressed in the cytosol. After PIP3 production, the PH domains translocate to the plasma membrane to bind with PIP3. Then, the co-localization of both luciferase fragments on the plasma membrane is triggered and active luciferases are recovered by complementation of luciferase fragments. The amount of translocated proteins is correlated to the amount of PIP3 that produced on the plasma membrane. As a result, the degree of PIP3 production is interpreted as quantified bioluminescence signals.

Next, we investigated the PIP3 production in subcellular compartments by controlling the PIP3 synthesis on organelle membranes using blue light. As described before, the synthesis of PIP3 is commonly stimulated by ligands with poor spatial regularity. However, the production of PIP3 on specific cellular membranes with high spatial resolution is extremely difficult. PIP3 is synthesized by PI 3-kinase from a precursor PIP2, which is much more abundant than PIP3 on the cell membranes. By using light sensitive CRY2-CIBN interaction, we engineered an optogenetic system that is able control the PIP3 synthesis on specific cell membranes. For this purpose, CIBN is predominantly expressed on distinct cellular membranes by genetically fusing a targeting sequence, whereas CRY2 is fused with constitutively active PI 3-kinase expressed in the cytosol. When cells expressing the two probes are irradiated with blue light, the CRY2 will be activated to interact with CIBN. Such interaction brings the active PI 3-kinase to cellular compartment to initiate the synthesis of PIP3 on specific subcellular membranes. On the other hand, light stimulation can also be applied to a more specific part of a cell to monitor localized PIP3 production.



## 1.5. References

1. Li, Z.; Venable, R. M.; Rogers, L. A.; Murray, D.; Pastor, R. W. *Biophys. J.* **2009**, *97* (1), 155-163.
2. DiNitto, J. P.; Cronin, T. C.; Lambright, D. G. *Sci. STKE* **2003**, *2003* (213), re16-.
3. Halet, G.; Viard, P.; Carroll, J. *Development* **2008**, *135* (3), 425-429.
4. Hoeller, O.; Kay, R. R. *Curr. Biol.* **2007**, *17* (9), 813-817.
5. Arai, Y.; Shibata, T.; Matsuoka, S.; Sato, M. J.; Yanagida, T.; Ueda, M. *Proc. Natl. Acad. Sci. U. S. A.* **2010**, *107* (27), 12399-12404.
6. Di Paolo, G.; De Camilli, P. *Nature* **2006**, *443* (7112), 651-657.
7. Weinkove, D.; Halstead, J.; Gems, D.; Divecha, N. *BMC Biol.* **2006**, *4* (1), 1.
8. Tengholm, A.; Meyer, T. *Curr. Biol.* **2002**, *12* (21), 1871-1876.
9. Gerisch, G.; Schroth-Diez, B.; Müller-Taubenberger, A.; Ecke, M. *Biophys. J.* **2012**, *103* (6), 1170-1178.
10. DiNitto, J. P.; Lambright, D. G. *Biochim. Biophys. Acta* **2006**, *1761* (8), 850-867.
11. Lietzke, S. E.; Bose, S.; Cronin, T.; Klarlund, J.; Chawla, A.; Czech, M. P.; Lambright, D. G. *Mol. Cell* **2000**, *6* (2), 385-394.
12. Czech, M. P. *Cell* **2000**, *100* (6), 603-606.
13. Dormann, D.; Weijer, G.; Dowler, S.; Weijer, C. J. *J. Cell Sci.* **2004**, *117* (26), 6497-6509.
14. Klarlund, J. K.; Tsiaras, W.; Holik, J. J.; Chawla, A.; Czech, M. P. *J. Biol. Chem.* **2000**, *275* (42), 32816-32821.
15. Niswender, K. D.; Gallis, B.; Blevins, J. E.; Corson, M. A.; Schwartz, M. W.; Baskin, D. G. *J. Histochem. Cytochem.* **2003**, *51* (3), 275-283.
16. Vasudevan, K. M.; Barbie, D. A.; Davies, M. A.; Rabinovsky, R.; McNear, C. J.; Kim, J. J.; Hennessy, B. T.; Tseng, H.; Pochanard, P.; Kim, S. Y.; Dunn, I. F.; Schinzel, A. C.; Sandy, P.; Hoersch, S.; Sheng, Q.; Gupta, P. B.; Boehm, J. S.; Reiling, J. H.; Silver, S.; Lu, Y.; Stemke-Hale, K.; Dutta, B.; Joy, C.; Sahin, A. A.;

- Gonzalez-Angulo, A. M.; Lluch, A.; Rameh, L. E.; Jacks, T.; Root, D. E.; Lander, E. S.; Mills, G. B.; Hahn, W. C.; Sellers, W. R.; Garraway, L. A. *Cancer Cell* **2009**, *16* (1), 21-32.
17. Clark, J.; Anderson, K. E.; Juvin, V.; Smith, T. S.; Karpe, F.; Wakelam, M. J. O.; Stephens, L. R.; Hawkins, P. T. *Nat. Meth.* **2011**, *8* (3), 267-272.
18. König, S.; Hoffmann, M.; Mosblech, A.; Heilmann, I. *Anal. Biochem.* **2008**, *378* (2), 197-201.
19. Oatey, P. B.; Venkateswarlu, K.; Williams, A. G.; Fletcher, L. M.; Foulstone, E. J.; Cullen, P. J.; Tavaré, J. M. *Biochem. J.* **1999**, *344* (2), 511-518.
20. Sato, M.; Ueda, Y.; Takagi, T.; Umezawa, Y. *Nat. Cell Biol.* **2003**, *5* (11), 1016-1022.
21. Poisson, J. *Rev. Hist. Pharm. (Paris)* **2010**, *58* (365), 51-56.
22. Niu, G.; Chen, X. *Theranostics* **2012**, *2* (4), 413.
23. Scott, D.; Dikici, E.; Ensor, M.; Daunert, S. *Annu. Rev. Anal. Chem.* **2011**, *4* (1), 297-319.
24. Min, J.-J.; Nguyen, V. H.; Kim, H.-J.; Hong, Y.; Choy, H. E. *Nat. Protoc.* **2008**, *3* (4), 629-636.
25. Nakajima, Y.; Yamazaki, T.; Nishii, S.; Noguchi, T.; Hoshino, H.; Niwa, K.; Viviani, V. R.; Ohmiya, Y. *PLoS ONE* **2010**, *5* (4), e10011.
26. Nakatsu, T.; Ichiyama, S.; Hiratake, J.; Saldanha, A.; Kobashi, N.; Sakata, K.; Kato, H. *Nature* **2006**, *440* (7082), 372-376.
27. Conti, E.; Franks, N. P.; Brick, P. *Structure* **1996**, *4* (3), 287-298.
28. Branchini, B. R.; Ablamsky, D. M.; Murtiashaw, M. H.; Uzasci, L.; Fraga, H.; Southworth, T. L. *Anal. Biochem.* **2007**, *361* (2), 253-262.
29. Troy, T.; Jekic-McMullen, D.; Sambucetti, L.; Rice, B. *Mol. Imaging* **2004**, *3* (1), 9-23.
30. Stirland, J.; Seymour, Z.; Windeatt, S.; Norris, A.; Stanley, P.; Castro, M.; Loudon, A.; White, M.; Davis, J. J. *Endocrinol.* **2003**, *178* (1), 61-69.
31. Zhang, W.; Purchio, A. F.; Chen, K.; Wu, J.; Lu, L.; Coffee, R.; Contag, P. R.; West, D. B. *Drug Metab. Dispos.* **2003**, *31* (8), 1054-1064.

32. Tamaru, T.; Hattori, M.; Ninomiya, Y.; Kawamura, G.; Varès, G.; Honda, K.; Mishra, D. P.; Wang, B.; Benjamin, I.; Sassone-Corsi, P.; Ozawa, T.; Takamatsu, K. *PLoS ONE* **2013**, *8* (12), e82006.
33. Tamaru, T.; Hattori, M.; Honda, K.; Benjamin, I.; Ozawa, T.; Takamatsu, K. *PLoS ONE* **2011**, *6* (9), e24521.
34. Saito, K.; Hatsugai, N.; Horikawa, K.; Kobayashi, K.; Matsu-ura, T.; Mikoshiba, K.; Nagai, T. *PLoS ONE* **2010**, *5* (4), e9935.
35. Dothager, R. S.; Flentje, K.; Moss, B.; Pan, M.-H.; Kesarwala, A.; Piwnicka-Worms, D. *Curr. Opin. Biotechnol.* **2009**, *20* (1), 45-53.
36. Ozawa, T.; Kaihara, A.; Sato, M.; Tachihara, K.; Umezawa, Y. *Anal. Chem.* **2001**, *73* (11), 2516-2521.
37. Ozawa, T.; Yoshimura, H.; Kim, S. B. *Anal. Chem.* **2012**, *85* (2), 590-609.
38. Takakura, H.; Hattori, M.; Takeuchi, M.; Ozawa, T. *ACS Chem. Biol.* **2012**, *7* (5), 901-910.
39. Kim, S. B.; Ozawa, T.; Watanabe, S.; Umezawa, Y. *Proc. Natl. Acad. Sci. U. S. A.* **2004**, *101* (32), 11542-11547.
40. Kim, S. B.; Umezawa, Y.; Kanno, K. A.; Tao, H. *ACS Chem. Biol.* **2008**, *3* (6), 359-372.
41. Hattori, M.; Haga, S.; Takakura, H.; Ozaki, M.; Ozawa, T. *Proc. Natl. Acad. Sci. U. S. A.* **2013**, *110* (23), 9332-9337.
42. Binkowski, B. F.; Butler, B. L.; Stecha, P. F.; Eggers, C. T.; Otto, P.; Zimmerman, K.; Vidugiris, G.; Wood, M. G.; Encell, L. P.; Fan, F.; Wood, K. V. *ACS Chem. Biol.* **2011**, *6* (11), 1193-1197.
43. Takeuchi, M.; Nagaoka, Y.; Yamada, T.; Takakura, H.; Ozawa, T. *Anal. Chem.* **2010**, *82* (22), 9306-9313.
44. Hida, N.; Awais, M.; Takeuchi, M.; Ueno, N.; Tashiro, M.; Takagi, C.; Singh, T.; Hayashi, M.; Ohmiya, Y.; Ozawa, T. *PLoS ONE* **2009**, *4* (6), e5868.
45. Deisseroth, K.; Feng, G.; Majewska, A. K.; Miesenböck, G.; Ting, A.; Schnitzer, M. *J. J. Neurosci.* **2006**, *26* (41), 10380-10386.
46. Yazawa, M.; Sadaghiani, A. M.; Hsueh, B.; Dolmetsch, R. E. *Nat. Biotechnol.* **2009**,

- 27 (10), 941-945.
47. Levskaya, A.; Weiner, O. D.; Lim, W. A.; Voigt, C. A. *Nature* **2009**, *461* (7266), 997-1001.
48. Kennedy, M. J.; Hughes, R. M.; Peteya, L. A.; Schwartz, J. W.; Ehlers, M. D.; Tucker, C. L. *Nat. Meth.* **2010**, *7* (12), 973-975.
49. Wu, Y. I.; Frey, D.; Lungu, O. I.; Jaehrig, A.; Schlichting, I.; Kuhlman, B.; Hahn, K. M. *Nature* **2009**, *461* (7260), 104-108.
50. Toettcher, J. E.; Gong, D.; Lim, W. A.; Weiner, O. D. *Nat. Meth.* **2011**, *8* (10), 837-839.
51. Yang, X.; Jost, A. P.-T.; Weiner, O.; Tang, C. *Mol. Biol. Cell* **2013**.
52. Loovers, H. M.; Postma, M.; Keizer-Gunnink, I.; Huang, Y. E.; Devreotes, P. N.; van Haastert, P. J. M. *Mol. Biol. Cell* **2006**, *17* (4), 1503-1513.
53. King, J. S.; Teo, R.; Ryves, J.; Reddy, J. V.; Peters, O.; Orabi, B.; Hoeller, O.; Williams, R. S. B.; Harwood, A. J. *Dis. Model. Mech.* **2009**, *2* (5-6), 306-312.
54. Park, W. S.; Do Heo, W.; Whalen, J. H.; O'Rourke, N. A.; Bryan, H. M.; Meyer, T.; Teruel, M. N. *Mol. Cell* **2008**, *30* (3), 381-392.
55. Boyden, E. S.; Zhang, F.; Bamberg, E.; Nagel, G.; Deisseroth, K. *Nat. Neurosci.* **2005**, *8* (9), 1263-1268.
56. Zhang, F.; Wang, L.-P.; Brauner, M.; Liewald, J. F.; Kay, K.; Watzke, N.; Wood, P. G.; Bamberg, E.; Nagel, G.; Gottschalk, A.; Deisseroth, K. *Nature* **2007**, *446* (7136), 633-639.
57. Chow, B. Y.; Han, X.; Dobry, A. S.; Qian, X.; Chuong, A. S.; Li, M.; Henninger, M. A.; Belfort, G. M.; Lin, Y.; Monahan, P. E.; Boyden, E. S. *Nature* **2010**, *463* (7277), 98-102.
58. Deisseroth, K. *Nat. Meth.* **2011**, *8* (1), 26-29.
59. Shimizu-Sato, S.; Huq, E.; Tepperman, J. M.; Quail, P. H. *Nat. Biotechnol.* **2002**, *20* (10), 1041-1044.
60. Tyszkiewicz, A. B.; Muir, T. W. *Nat. Meth.* **2008**, *5* (4), 303-305.
61. Leung, D. W.; Otomo, C.; Chory, J.; Rosen, M. K. *Proc. Natl. Acad. Sci. U. S. A.* **2008**, *105* (35), 12797-12802.

62. Cashmore, A. R. *Cell* **2003**, *114* (5), 537-543.
63. Sancar, A. *Chem. Rev.* **2003**, *103* (6), 2203-2238.
64. Chaves, I.; Pokorny, R.; Byrdin, M.; Hoang, N.; Ritz, T.; Brettel, K.; Essen, L.-O.; van der Horst, G. T. J.; Batschauer, A.; Ahmad, M. *Annu. Rev. Plant Biol.* **2011**, *62* (1), 335-364.
65. Liu, H.; Yu, X.; Li, K.; Klejnot, J.; Yang, H.; Lisiero, D.; Lin, C. *Science* **2008**, *322* (5907), 1535-1539.
66. Liu, H., Liu, B., Zhao, C., Pepper, M., & Lin, C. *Trends. Plant Sci.* **2011**, *16*(12), 684-691.

## 2. Development of Bioluminescence Probes for the Analysis of PIP3 on the Cell Membrane

### 2.1. Introduction

Phosphatidylinositol (3,4,5)- trisphosphate (PIP3) is a pivotal lipid second messenger that mediates central cellular events. In normal conditions, the amount of PIP3 is strictly balanced by the actions of PI 3-kinase that synthesizes PIP3 and phosphatases that degrade the PIP3. On the contrary, the overall elevated PIP3 level induces continuous activation of infinite cell growth and inhibition of the signal pathways for apoptosis. Such dysfunctions of PIP3 metabolism are found in cancer cells. Although the PIP3 is known to be involved in fatal diseases, the detailed mechanism of its regulative role remains unclear due to limitations of PIP3 analytical methods.

The existing in vitro methods includes analysis using PIP3-specific antibodies for the assessment of total PIP3 amount in the cells and instrumental analysis that measures the absolute quantity of PIP3. These methods are insufficient for evaluating PIP3 in the actual biological context and they suffer from inaccurate measurements caused by destructive sample pretreatment. On the other hand, live cell fluorescence imaging has been developed to visualize the PIP3 dynamics in living cells. Such in vivo analyses of PIP3 using fluorescent probes are able to provide valuable informations of PIP3 dynamics in single cells. However, limitation exists as the fluorescent probes are inconvenient for the larger scale analysis, which is indispensable for further applications, caused by the intricate equipment for microscopic observations. More extensive analysis of PIP3 such as spatiotemporal analysis of PIP3 and quantitative

analysis of PIP3 is required by the needs for further studying the PIP3 functions and facilitating medical applications of PIP3. Therefore, spatiotemporal analysis of PIP3 amount is of vital importance to further elucidate the biological functions of PIP3 and to clarify the PIP3 regulative roles to diseases.

Herein, we are developing a probe to analyze the relative amount of PIP3 molecules on the plasma membrane using split luciferase complementation. We combine the use of Pleckstrin Homology domain of GRP1 (general receptor for phosphoinositides 1) as a PIP3 recognition module with the split-luciferase complementation technology. The scheme for the bioluminescence analysis of PIP3 is shown in Figure 2-1A. In our design, N-terminal luciferase fragment is anchored on the plasma membrane (LucN-pm), whereas C-terminal luciferase fragment is fused with tandem PIP3 binding motifs (PP-LucC), which localize in the cytosol. The PIP3 binding motifs, the tandem PH domains, are used to sense PIP3 production and to bring the PP-LucC from the cytosol to the plasma membrane, where luciferase fragment complementation is initiated by the co-localization of LucN-pm and PP-LucC. The bioluminescence thus generated is proportional to the relative amount of PIP3 on the plasma membrane. We also demonstrated that the bioluminescent probes were applied to a high-throughput screening system and bioluminescence imaging.

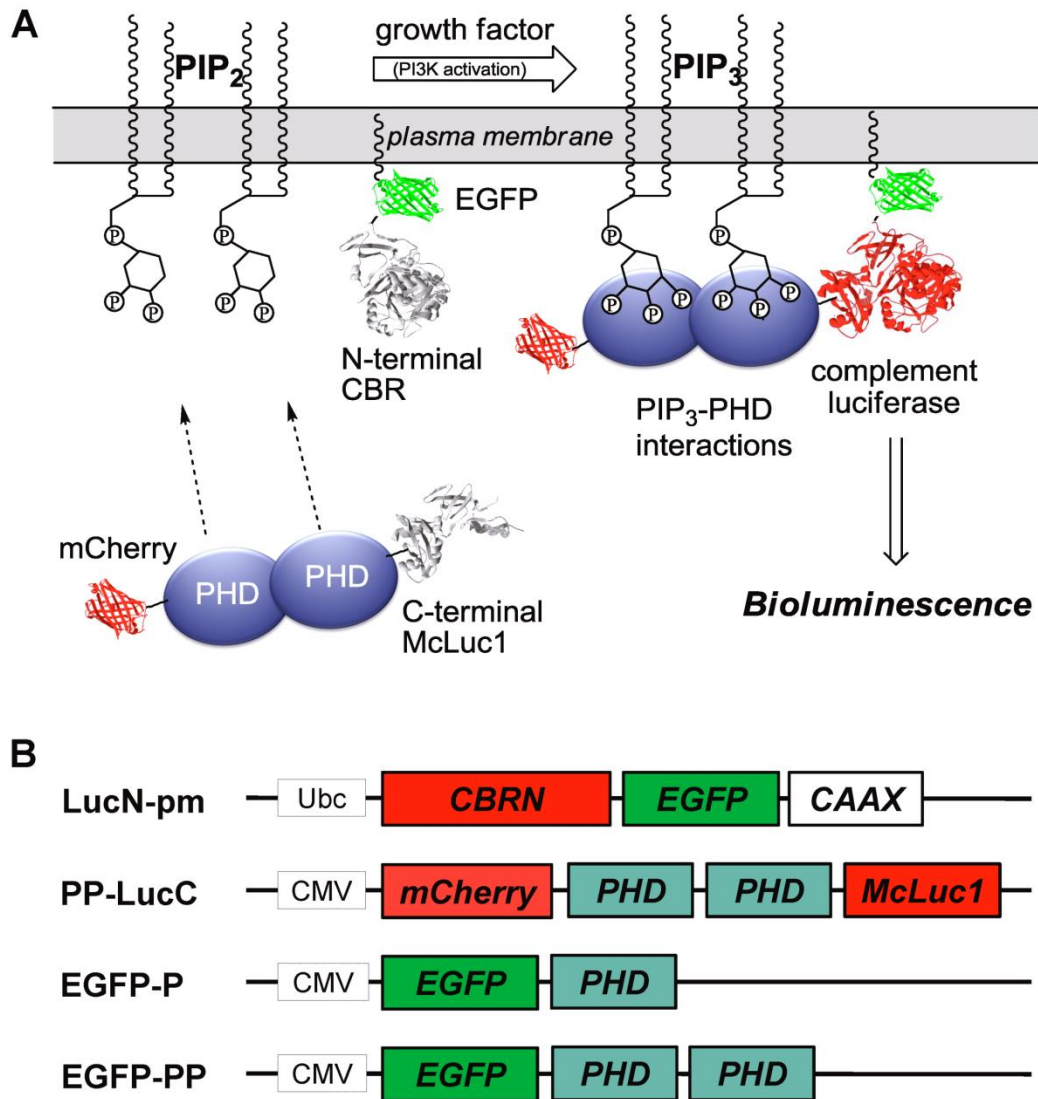


**Figure 2-1.** (A) Schematics for the detection of membrane PIP3. An N-terminal fragment of CBR is anchored predominantly on the plasma membrane (LucN-pm). A C-terminal luciferase fragment (McLuc1) connected with tandem PH domains (PHD) is expressed in cytosol (PP-LucC). When PIP3 is produced on the plasma membrane, PP-LucC migrates to the plasma membrane through the binding of PHDs to PIP3, resulting in a reconstitution of the luciferase fragments and recovery of bioluminescence. EGFP and mCherry are fused respectively in LucN-pm and PP-LucC for fluorescence observation of the probe localizations. (B) Schematics for domain structures of PIP3 probes. All text in *italics* refers to the genes of their corresponding proteins. CMV and Ubc are promoters, presented in expression vectors with different selection markers, for high-level gene expressions in mammalian cells. PHD represents pleckstrin homology domain from GRP1. EGFP and mCherry are green and red fluorescent proteins. CAAX is a polybasic plasma membrane localization signal of KRas4B (KKKKKKSKTKCVIM).

## 2.2. Experimental Section

### 2.2.1. Materials

The cDNA library of human brain, a DNA polymerase (PrimSTAR), restriction enzymes were purchased from Takara Bio Inc. (Ohtsu, Shiga, Japan). Platelet derived growth factor receptor type B (PDGFRB) cDNA was obtained from DNAFORM Precision Gene Technologies (Kanagawa, Japan). Expression vectors for mammalian cell lines pcDNA4/V5-His (B), pcDNA3.1/myc-His (B), and pUB6/V5-His (B) were obtained from Life Technologies Inc. (Carlsbad, CA). Dulbecco's modified Eagle's medium/Nutrient Mixture F12 (DMEM/Ham's F-12) and 0.05% trypsin-EDTA were obtained from Wako Pure Chemical Industries Ltd. (Osaka, Japan), fetal bovine serum (FBS), and penicillin–streptomycin were purchased from Gibco (Grand Island, N.Y.). Lipofectamine LTX, Geneticin (G418), Zeocin, and Blastidicin S HCl were purchased from Life Technologies Inc. D-Luciferin potassium salt was obtained from Wako Pure Chemical Industries Ltd. Luciferase assay kit Bright-Glo Luciferase Assay System was purchased from Promega Corp. (Madison, WI). Human recombinant PDGF bb was obtained from R&D Systems (Emeryville, CA). Wortmannin was purchased from Sigma Chemical Co. (St. Louis, MO). Rabbit anti-GFP antibody and rabbit anti-RFP antibody were purchased, respectively, from Clontech (Palo Alto, CA) and Santa Cruz Biotechnology Inc. (Santa Cruz, CA). Mouse anti- $\beta$ -actin antibody was obtained from Sigma. Anti-rabbit IgG antibody and anti-mouse IgG antibody labeled with horseradish peroxidase (HRP) were obtained from Jackson Immuno Research Laboratories, Inc. (West Grove, PA).

### 2.2.2. Construction of Plasmids for Mammalian Cell Expression

All genes were amplified by standard polymerase chain reaction (PCR) using PrimeSTAR DNA polymerase and customized specific primers. cDNAs of Click Beetle

Red (CBR) luciferase and multiple-complement luciferase fragment- common C-terminal (McLuc1) were used as the template to generate LucN (1-413 amino acids of CBR) and McLuc1.<sup>1</sup> cDNAs of EGFP and mCherry were used as templates to amplify genes coding corresponding fluorescent proteins. The cDNA of PH domain (GRP1) was amplified from human brain cDNA library. PDGFRB gene was amplified using the purchased cDNA as the template.

All genes were subcloned into mammalian expression vectors using specific restriction enzyme sites. DNA coding a polybasic CAAX motif of KRas4B (KKKKKKSKTKCVIM) was prepared by annealing oligo DNAs with the corresponding sequence,<sup>2</sup> and ligated into an expression vector. Sequences of all inserted genes and CAAX motif were verified using specific primers and BigDye Terminators v3.1 cycle sequencing kit and a genetic sequencer (ABI Prism 310 Genetic Analyzer; GE Healthcare). Fusion protein of EGFP-PHD (GRP1) (EGFP-P) was produced to verify production of PIP3.<sup>3</sup>

### 2.2.3. Cell Culture and Preparation of Stable Cell Line

The Chinese hamster ovary (CHO-K1) cell line was kept in DMEM/Ham's F-12 (high glucose) supplemented with 10% FBS, 100 unit/mL penicillin, and 100 µg/mL streptomycin in 10 cm plastic dishes. It was incubated at 37 °C in 5% CO<sub>2</sub> atmosphere. Cells were subcultured into new plastic dishes every three days. Plasmids with the DNA of fusion proteins were introduced to CHO cells using transfection reagent Lipofectamine LTX. Briefly, 2 µg of cDNA was mixed with 5 µL of Lipofectamine LTX reagent and was added to 200 µL Opti-MEM. The mixture was then added to cultured cells in 3.5 cm plastic dishes 20 min after mixing. A stable cell line expressing PDGF receptor beta type was established (CHO-PDGFR) from a single cell colony obtained by a selective marker of Zeocine (100 µg/mL). This cell line was used in all subsequent

experiments and screenings. The established cell line can produce PIP3 because dimerization and phosphorylation of PDGF receptor recruits and activates PI 3-kinase that synthesizes PIP3.<sup>4</sup> Geneticin (G418) (1.2 mg/mL) and Blasticidin (10 µg/mL) were used for screening a cell line that respectively harbors pPP-LucC/pP-LucC (pcDNA3.1/myc-His (B)) and pLucN-pm (pUB6/V5-His (B)).

## 2.2.4. Validation of the Production of PIP3 in CHO-PDGFR cell line

### 2.2.4.1. Immunostaining

The CHO-PDGFR cells were seeded in a cover glass in 3.5 cm plastic dishes. Medium was changed to a serum-free medium and incubated for 3 h. Cells were stimulated with 50 ng/mL PDGF. Hoechst (Invitrogen) was added to stain the nucleus. Five min after the PDGF stimulation, cells were washed with PBS(+), fixed in 4% paraformaldehyde in PBS at RT for 10 min, permeated with 0.2% Triton X-100 for 5 min at RT, incubated with mouse anti-PIP3 antibody (IgM) (Invitrogen) for 1 h, and stained with Alexa488 conjugated goat anti-mouse IgM (Invitrogen) for 1 h. After each incubation, cells were washed 3 times by PBS (+) and 0.2% FSG by shaking. The cells with or without PDGF stimulation were visualized by a laser scanning confocal microscopy (IX81-FV1000-D; Olympus Corp., Tokyo, Japan) equipped with a 60× oil immersion objective, and obtained images were analyzed using a software (FV10-ASW; Olympus Corp.) (Fig. 2-2).

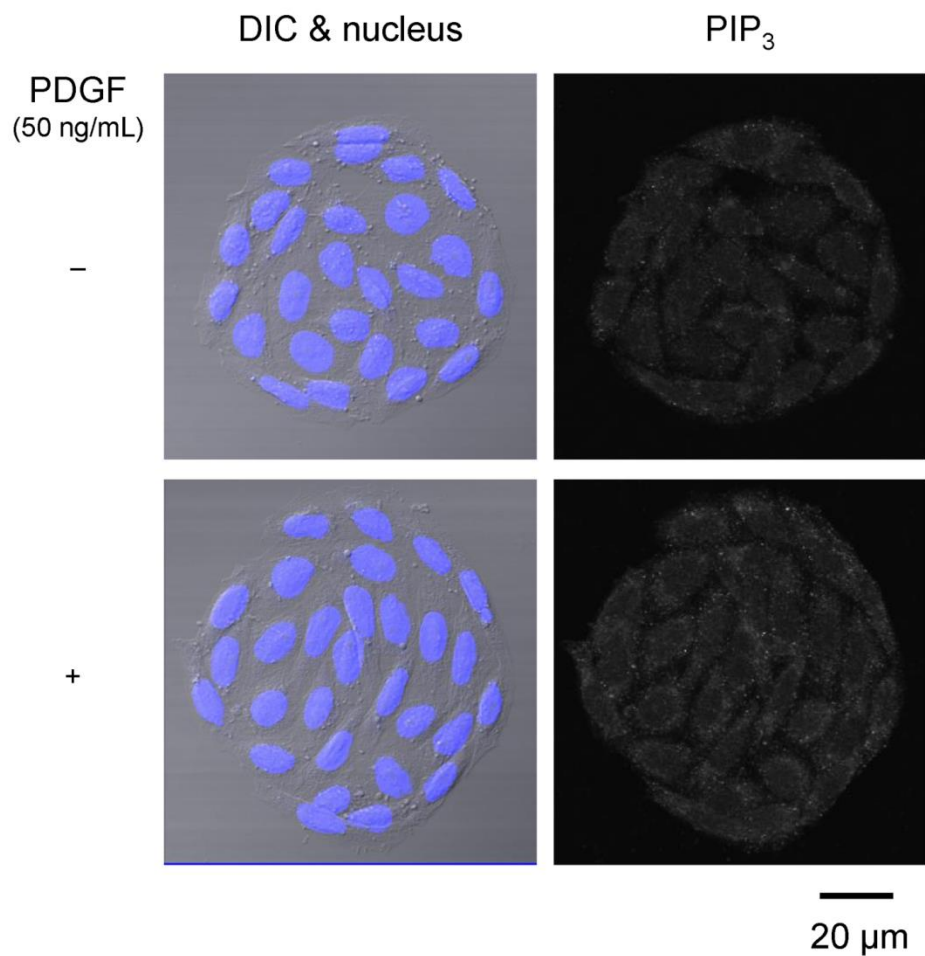


**Figure 2-2.** Immunostaining of PIP<sub>3</sub> with its specific antibody. CHO-PDGFR cells in the presence and absence of 50 ng/mL PDGF were fixed with PFA, permeated with a detergent, and then blotted by a PIP<sub>3</sub> antibody. Alexa488 conjugated with a second antibody was used for imaging PIP<sub>3</sub> under a confocal microscopy. Nucleus of the cells was stained with Hoechst before stimulation. Scale bar: 20 μm.

#### 2.2.4.2. Protein Translocation

The CHO-PDGFR cells transiently expressing EGFP-P probe were seeded in a cover glass in 3.5 cm plastic dishes. Medium was changed to a serum-free medium without phenol red and incubated for 2 h. Cells were observed under the fluorescence confocal microscopy. Fluorescence images were captured before and after cells were stimulated with 50 ng/mL PDGF by the fluorescence confocal microscopy (Fig. 2-3).

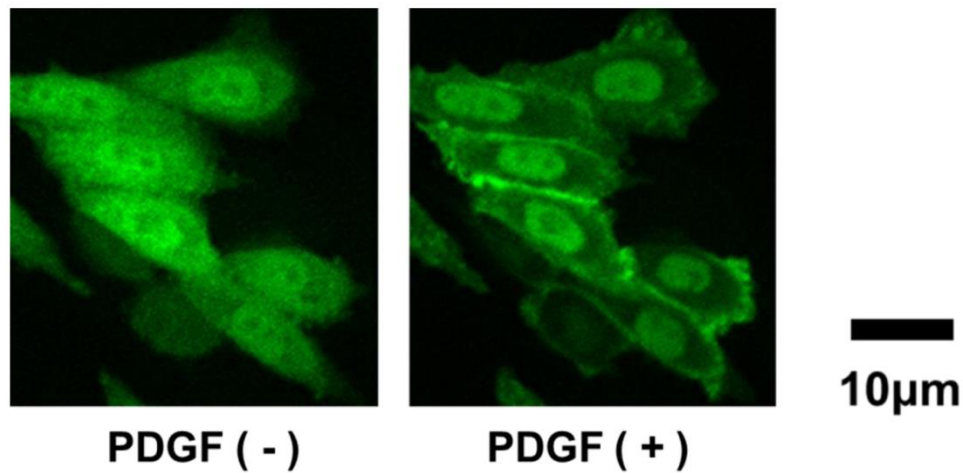


**Figure 2-3.** Validation of the production of PIP3 in the CHO-PDGFR cells. The PIP3 indicator, EGFP-PHD (EGFP-P), was expressed in CHO-PDGFR cells. 30 ng/mL PDGF was added to the cells. The translocation of EGFP-P was observed using fluorescence confocal microscopy. Scale bar: 10  $\mu$ m.

## 2.2.5. Evaluation of the Bioluminescent Probes for PIP3 analysis

### 2.2.5.1. Immunoblot Analysis

The cell lysate of PP-LucC and LucN-pm-expressing CHO-PDGFR and wild type CHO (CHO-K1) was subjected to SDS-PAGE using 8% polyacrylamide gel. The proteins in the gel were transferred to a nitrocellulose membrane. The membrane was blotted with a polyclonal anti-GRP or an anti-RFP antibody, and then incubated with a HRP conjugated anti-rabbit antibody for detection. After detection, the membrane was stripped and then probed again by an anti- $\beta$ -actin antibody with subsequent probing with an HRP conjugated anti-mouse IgG antibody for the control imaging of  $\beta$ -actin. Western blot images were captured using an image analyzer (LAS-1000 plus; Fuji Film Co., Tokyo, Japan) with a chemiluminescence system (ECL prime; GE Healthcare, Little Chalfont, Buckinghamshire, UK).

### 2.2.5.2. Imaging of Probe Dynamics by Fluorescence Confocal Microscopy

The dynamics of single PH domain and tandem PH domains in response to PIP3 production were compared. CHO-PDGFR cells expressing either EGFP-P or EGFP-PP were subcultured to glass-based dishes and incubated for 2 days. The cells were then incubated for 3 h in the serum-free medium in order to eliminate possible agonists or inhibitors from the medium. This procedure is necessary for precise analysis of the chemical effects on PIP3 production. Synthesis of PIP3 was induced by adding 60 ng/mL PDGF to the CHO-PDGFR cells. Fluorescence time-lapse images were captured using the laser scanning confocal microscope. We obtained EGFP-P and EGFP-PP translocation dynamics with intervals of 30 s for 1 h (Fig. 2-4). Cellular localizations of LucN-pm and PP-LucC before and after PIP3 production stimulated by 20% serum (FBS, final concentration), which activate PI 3-kinase,<sup>5</sup> were visualized (Fig. 2-5).

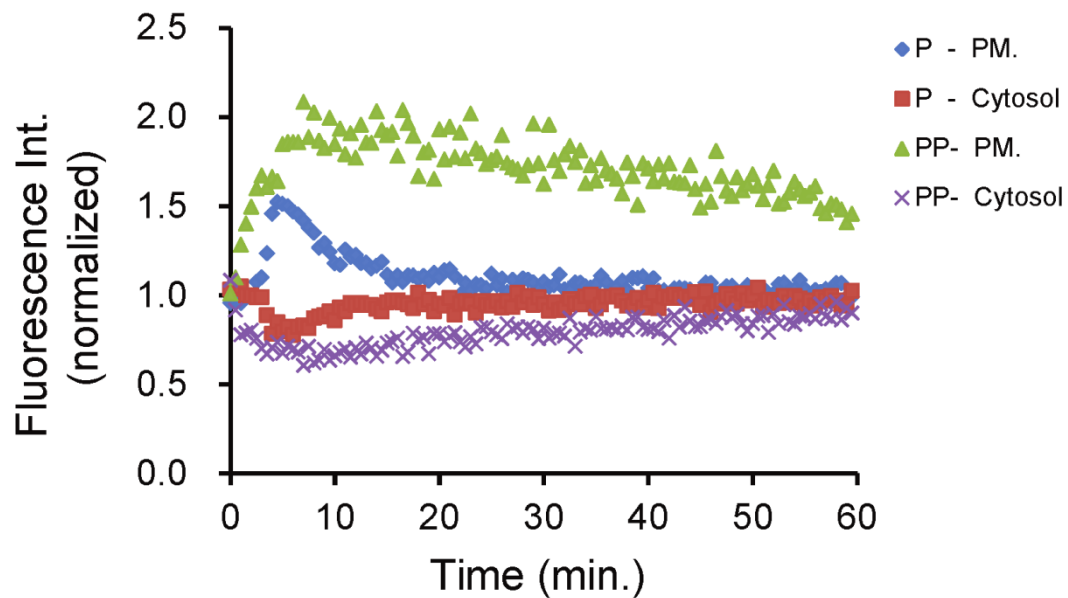


**Figure 2-4.** Time-dependent comparison between EGFP-P and EGFP-PP translocations upon PIP3 production. Dynamics of single PH domain and tandem PH domains were compared using time-lapse confocal imaging under the stimulation of 60 ng/mL PDGF. Images were taken every 30 s. The plasma membrane and cytosolic areas for each probe were selected. The intensities of each area were obtained. Time-lapse translocations were calculated based on fluorescence signals on the plasma membrane or in the cytosol (EGFP-P, n=9; EGFP-PP, n=6). The fluorescence intensities were normalized through the division by the average fluorescence of each cell at every time point.

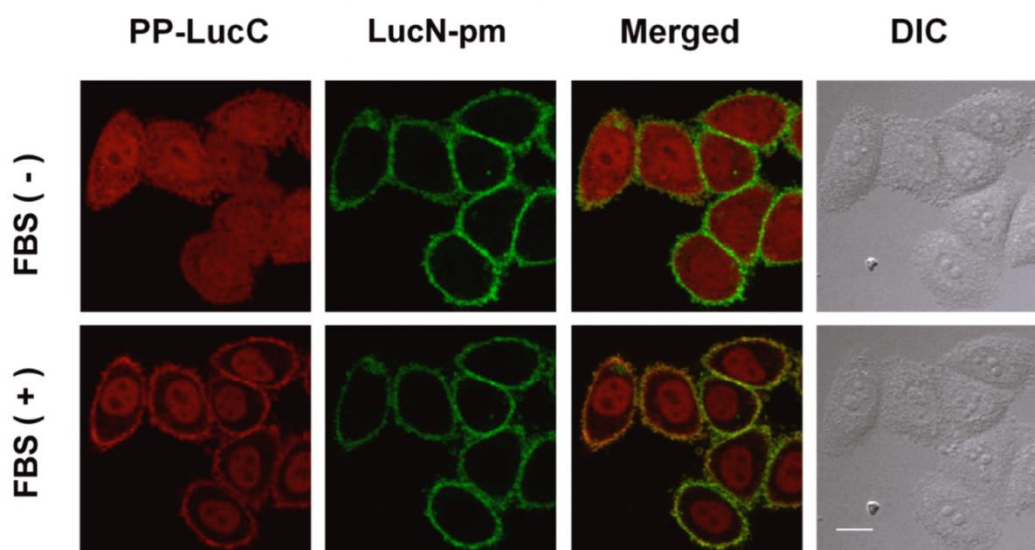


**Figure 2-5.** Identification of the probe localizations using confocal imaging. CHO-PDGFR cells stably expressing PP-LucC and LucN-pm were starved for 3 h before imaging. Cells added with 20% serum were incubated for 10 min before obtaining an image. Localizations of PP-LucC (red) and LucN-pm (green) with and without serum are shown. Scale bar: 10  $\mu$ m.

### 2.2.5.3. Real-time Bioluminescence Assay for PIP3 in Live Cells

CHO-PDGFR cells expressing LucN-pm and PP-LucC were cultured in 35 mm dishes. They were then starved for 3 h in serum-free medium. D-Luciferin was added to the medium to reach a final concentration of 5 mM. The dishes were then set on a dish-type photon countable incubator AB-2550 Kronos (ATTO Corp., Tokyo, Japan). Bioluminescence was measured every 1 min at 37°C with an exposure time of 10 s. For the inhibition of PIP3 production, 21 ng/mL wortmannin was added to the cells 30 min before the addition of a PIP3 agonist. The 20% serum was added to cells for the activation of PIP3 production. Results are presented in Figure 2-6.

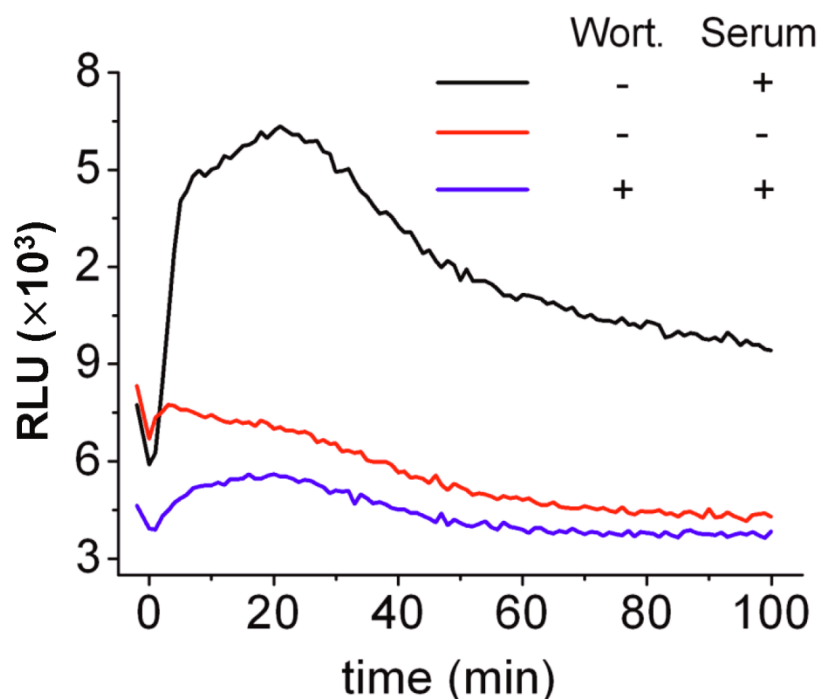


**Figure 2-6.** Real-time bioluminescence analyses for PIP3 production. CHO-PDGFR cells expressing PP-LucC and LucN-pm were pretreated with the PI 3-kinase inhibitor 21 ng/mL wortmannin and were then stimulated with 20% serum. Bioluminescence signals were recorded every 2 min with an exposure time of 10 s.

#### 2.2.5.4. Bioluminescence Assays in Lysed Cells

A Dual-Glo® Luciferase Assay System (Promega Corp, Madison, WI) was used to obtain the relative luminescence unit (RLU) of reconstituted luciferase and that of an internal control, the Renilla luciferase (RLuc). The Dual-Glo and Bright-Glo reagents provide a lysis buffer to permeate the cell membrane and to prevent cellular proteins from decomposition. It is known empirically that in such a mild condition with the lysis buffer, reconstituted luciferase maintains its activity for more than 10 min.<sup>6</sup> Thus, the reagents are useful for quantitative evaluation of bioluminescence using a 96 well plate assay format. In all experiments, RLU of the reconstituted luciferase was divided by that of RLuc, of which value was designated as RLU ratio. CHO-PDGFR cells

expressing both probes were seeded in a 10 cm plastic dish, and were transfected with 0.5  $\mu\text{g}$  pGL4.74 [hRlucP] Vector (Promega). The cells were then grown on a 96-well microtiter plate for 1 day. The medium was changed into a serum-free medium 3 h prior to the assays. Cells were pretreated with an inhibitor, 0.21  $\mu\text{g}/\text{mL}$  wortmannin, for 1 h, and then stimulated with either 50 ng/mL PDGF or 10% serum. After 25 min, 50  $\mu\text{L}$  of Dual-Glo was added to each well. Bioluminescence signals were recorded by the plate reader with the exposure time of 5 s per well. Fifty  $\mu\text{L}$  of the Stop&Glo reagent was added to each well to quench the reconstituted luciferase activity and to measure RLuc bioluminescence. Results of RLU ratio (reconstituted luciferase/RLuc) were shown in Figure 2-7, indicating activation and inhibition of PIP3.

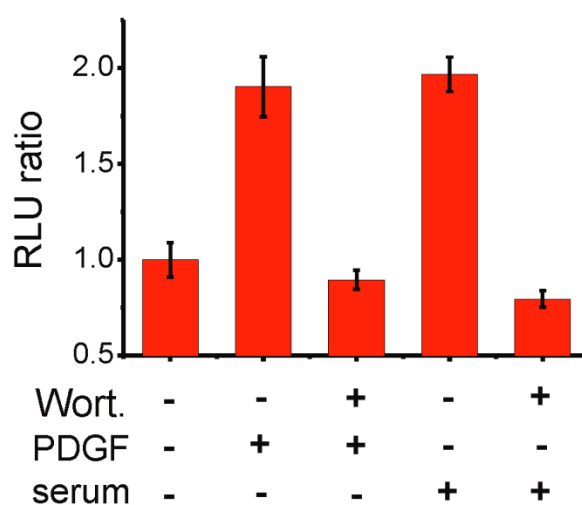


**Figure 2-7.** Activation and inhibition of the production of PIP3. The cells expressing PP-LucC, LucN-pm and RLuc were pretreated with the PI 3-kinase inhibitor of wortmannin (0.21  $\mu\text{g}/\text{mL}$ ) and stimulated with 10% serum. Twenty five min after serum addition, cells were subjected to the dual luciferase assay. The RLU ratios (reconstituted luciferase/RLuc) were obtained and normalized against the RLU ratios of control cells (n=3).

### 2.2.5.5. Investigation of Probe Reversibility

CHO-PDGFR cells expressing both probes were seeded on a 96-well microtiter plate. The medium was changed to a serum-free medium 3 h before assays. A Bright-Glo™ Luciferase Assay System (Promega) was used to loosen the cell membrane structure and to provide the D-luciferin. Briefly, 50 ng/mL PDGF was added sequentially every 1 h into different wells and incubated for 30 min. The depletion of PDGF was performed by washing and exchanging the medium into a serum-free type. The activation and washing steps of different wells set varied incubation times from 0 - 6 h after the PDGF depletion. Next, a second stimulation of PDGF was performed every 1 h to different wells that have already been depleted of PDGF for 6 h. The medium was again washed and replaced by a new one without PDGF, and incubated for 0 - 4 h. Finally, 50 µL Bright-Glo was added to obtain the bioluminescence using a 96-well microplate reader (TriStar LB941; Berthold Technologies GmbH and Co. KG, Germany). Results of the assays for reversibility are shown in Figure 2-8.

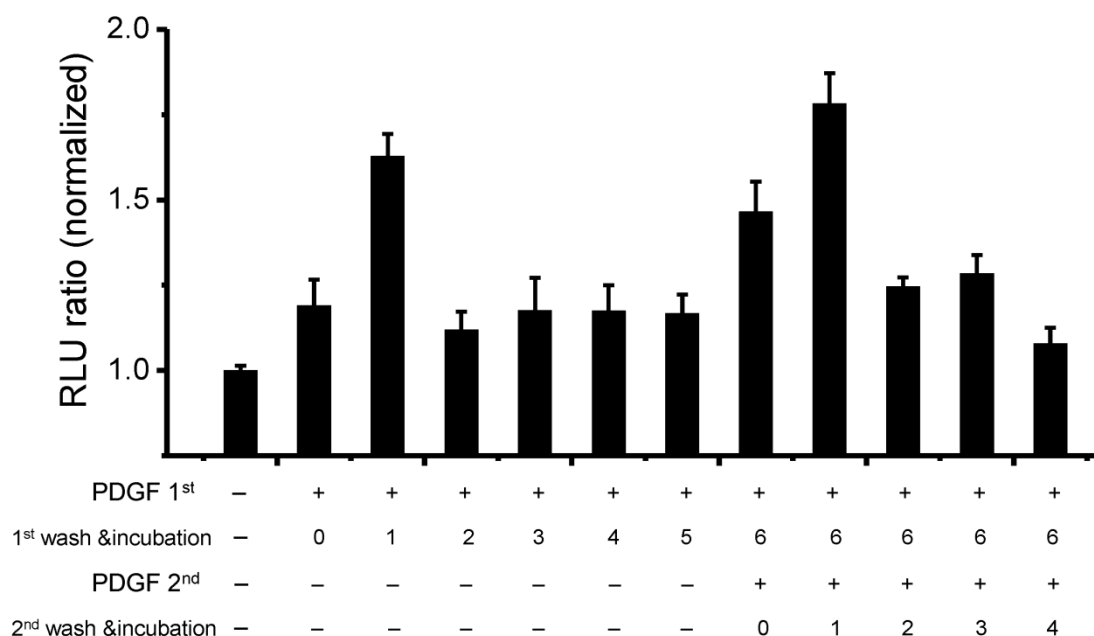


**Figure 2-8.** Reversibility of the bioluminescent probes upon repeated stimulation and depletion of PDGF. CHO-PDGFR cells expressing both probes were prepared in a 96-

well microtiter plate. The cells were activated with 50 ng/mL PDGF for 30 min, and then inactivated by depletion of PDGF through the exchanging of medium. A second stimulation by 50 ng/mL PDGF and its depletion was performed under the same condition as the first trial. Bioluminescence was recorded using a plate reader with the exposure time of 5 s/well, and RLU ratios (reconstituted luciferase/Rluc) are shown (n=3).

## 2.2.6. Bioluminescence Assays of PIP3 Production

### 2.2.6.1. Comparison between Bioluminescence Intensities in Live Cell and Lysed Cell Assays

CHO-PDGFR cells stably expressing PP-LucC and LucN-pm were seeded in a 96-well microtiter plate and were allowed for growth for 48 h. For the live cell assays, the medium was replaced by a serum-free medium and the cells were incubated for 1.5 h. The medium was then changed into a medium which contains 5 mM D-luciferin and incubated for 1.5 h. PDGF (100 ng/mL) was added for 25 min. The bioluminescence signals were directly obtained. For the lysis assays, medium was changed to the serum-free medium and incubated for 3 h. PDGF (100 ng/mL) was added for 25 min. Bioluminescence signals were produced by mixing 50  $\mu$ L Bright-Glo reagent into all wells and signals were obtained after 5 min incubation. (Exposure time for all measurement: 1 s, n=3)

### 2.2.6.2. Quantitative Analyses for the Effects of PIP3 Agonist and Inhibitor

For the quantitative analysis of an agonist for PIP3 production, cells expressing both probes and Rluc were prepared 1 day before the assay in a 96-well microtiter plate. The medium was changed to a serum-free medium 3 h before assays. Different

concentrations of PDGF (0.01, 0.1, 1, 10, 50, and 200 ng/mL) were added to investigate dose-dependent bioluminescence signals induced by agonist effects of PIP3 production. After 25 min incubation, 50  $\mu$ L Dual-Glo was added to obtain the RLU of reconstituted luciferase using the plate reader. Then, the RLU of Rluc was acquired by addition of 50  $\mu$ L Stop&Glo. The RLU ratio (reconstituted luciferase/Rluc) of each well was calculated. For the quantitative analysis of inhibitors, cells expressing both probes were pretreated with a PI 3-kinase inhibitor, wortmannin, with different concentrations from 4.3 pg/mL to 0.43  $\mu$ g/mL. After 1 h, the cells were stimulated with either 50 ng/mL PDGF or 10% serum, and incubated for 25 min. RLU values of reconstituted luciferase and Rluc were obtained sequentially by the dual assay system. The quantitative activation and inhibitory effects are shown in Figure 2-9.

### 2.2.6.3. Time-dependent Bioluminescence Signals with the Lysis Buffer

CHO-PDGFR cells expressing PP-LucC and LucN-pm were prepared in a 96-well microtiter plate and allowed growth for 48 h. Cells were then incubated in the serum-free medium for 3 h. Different concentrations of PDGF were added into each well. Twenty five minutes later, 50  $\mu$ L Bright-Glo was added. After the cells were exposed to the Bright-Glo buffer for 5, 10, 15, 20, 30 and 40 min, bioluminescence signals were obtained by a plate reader (exposure time: 1 s). The signals of each duration time for the Bright-Glo incubation were analyzed and EC<sub>50</sub> values were acquired by the curve fitting. A time-dependent curve for the decay of bioluminescence was also obtained within 50 minutes (n=18).

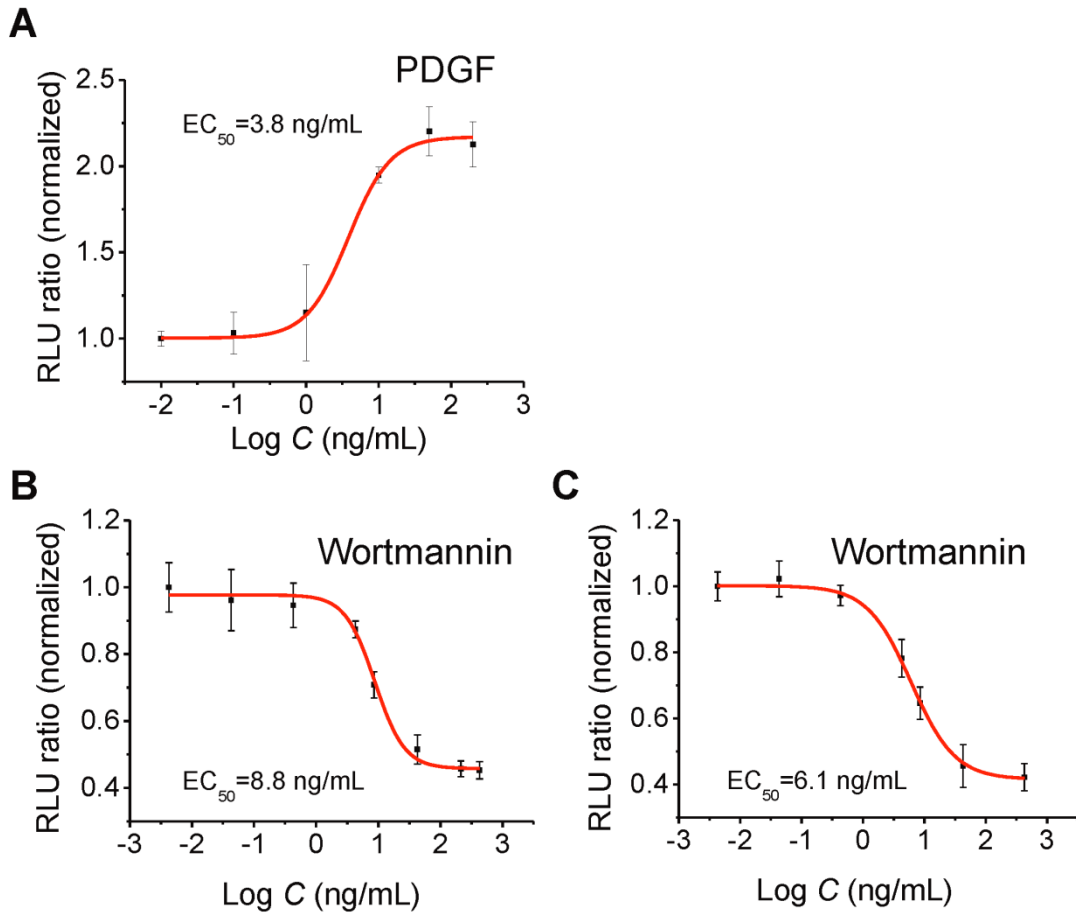


**Figure 2-9.** Analyses of PIP3 production induced by agonists and an inhibitor. (A) Concentration-dependent induction of PIP3 by an agonist, PDGF. PDGF was added to CHO-PDGFR cells expressing PP-LucC, LucN-pm and RLuc to final concentrations of 0.01, 0.1, 1, 10, 50, and 200 ng/mL. The bioluminescence signals of the reconstituted luciferase and RLuc were obtained thereafter. The RLU ratios were normalized against those of 0.01 ng/mL PDGF stimulated cells (n=3). (B) Concentration-dependent inhibition of PIP3 by an inhibitor against PDGF activation. Cells were pretreated with different concentrations of wortmannin for 1 h, and were subsequently stimulated with 50 ng/mL PDGF. The signals of reconstituted luciferase and RLuc were obtained 25 min after addition of PDGF. The RLU ratios were calculated and normalized against the RLU ratios of wortmannin (4.3 pg/mL) treated cells (n=3). (C) Concentration dependent bioluminescence reduction by wortmannin against serum activation. Cells pretreated with different wortmannin concentrations in (B) were stimulated with 10% serum for 25 min. Signals of reconstituted luciferase and RLuc were recorded and the RLU ratios were calculated. The values were normalized against that of wortmannin (4.3 pg/mL) treated cells (n=3).

### 2.2.7. Validation of a High-throughput Screening System

CHO-PDGFR cells that stably expressing both PP-LucC and LucN-pm were prepared in a 96-well microtiter plate 48 h before assay with an initial cell density of 20,000–40,000 cells/well. Medium was changed to serum and phenol-red free DMEM/F-12 7 h before assays. For validation of HTS of PIP3 agonist, 10% serum was added to the middle wells as positive control, whereas the same volume of DMEM/F-12 was added to the flanking 16 wells as negative control. Thirty minutes after stimulation, 40  $\mu$ L Bright-Glo was mixed in each well. Then bioluminescence signals were recorded using a 96-well microplate reader with an exposure time of 0.1 s/well. For validation of HTS of PIP3 inhibitor, 86 ng/mL wortmannin was added to the middle wells of plate for inhibitor pretreatment as positive control, whereas the same volume of DMEM/F-12 as that of wortmannin was added to pretreat the flanking wells as negative control. We added 10% serum to all wells. Thirty minutes after stimulation, 40  $\mu$ L Bright-Glo was mixed in each well and bioluminescence signals were acquired. The background signal was measured before the assay and subtracted from the final data. Based on bioluminescence signals in an entire plate, several parameters for HTS were evaluated. Implications and formulae related to the parameters are shown as follows.

Av100% represents the average value for positive control wells. Av0% denotes the average value for negative control wells. CV stands for the coefficient of variation. S/B stands for the signal/background ratio.

$$S/B = Av_{100\%}/Av_{0\%}$$

The *Z'* factor indicates the quality of a high-throughput screening assay.<sup>7</sup>

$$Z' \text{ factor} = 1 - \frac{(3 \times SD_{100\%} + 3 \times SD_{0\%})}{|Av_{100\%} - Av_{0\%}|}$$

The assay was repeated twice to ensure reproducibility.

## 2.2.8. Visualization of PIP3 Production by a Bioluminescence Microscopy

CHO-PDGFR cells expressing LucN-pm and PP-LucC were starved in serum-free medium for 3 h before imaging. D-Luciferin was added to be 5 mM and was pre-incubated for 1 h. The cells were stimulated by addition of 10% serum. Bioluminescence images were recorded using an upright bioluminescence microscope (BX61; Olympus Corp.) with a 20× water dipping objective (0.40 NA). We used only an emission long-pass filter, which allows through light above 420 nm, covering bioluminescence signals from most types of luciferases. Digital images were obtained using a cooled (set at  $-80^{\circ}\text{C}$ ) electron-multiplying charge-coupled device (EM-CCD) camera (ImagEM-1K; Hamamatsu Photonics KK, Japan). The filters and camera control were adjusted automatically using software (MetaMorph; Universal Imaging Corp., Downingtown, PA). Images were taken with an exposure time of 10 min for bioluminescence and 300 ms for differential interference contrast images (Fig. 2-10).

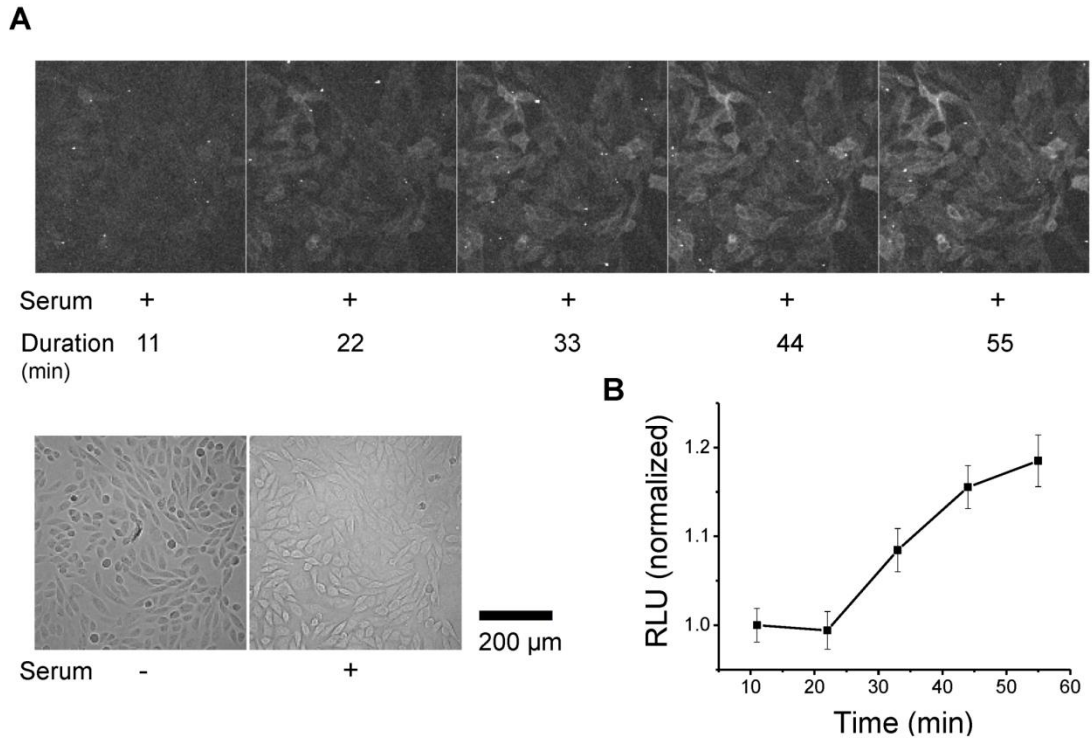


**Figure 2-10.** Visualization of PIP3 production in living cells using a bioluminescence microscopy. CHO-PDGFR Cells that expressed PP-LucC and LucN-pm were incubated in serum-free medium for 3 h and then stimulated with 10% serum. One hour before imaging, D-luciferin was added to the medium to reach a final concentration of 5 mM. (A) Bioluminescence and differential interference contrast (DIC) images acquired after addition of the serum. The exposure times for luminescence and DIC images were 10 min and 300 ms, respectively. The montage figures show time-lapse images indicating an increase in PIP3 by serum activation. The two DIC images below show images before and after stimulation. Scale bar: 200  $\mu$ m. (B) Quantified bioluminescence from the time-lapse images. Several areas were selected in the images to evaluate average RLU (n=7).

## 2.3. Results and Discussion

### 2.3.1. Schematics for the PIP3 Detection and Design of Fusion Proteins

The schematics for PIP3 analysis and fusion protein structures are shown in Figure 2-1(A) and 2-1(B), respectively. The PIP3 probes using split luciferase fragments was composed of a pair of protein modules. One is an N-terminal luciferase fragment (1–415 amino acids of a click beetle luciferase red mutant, CBR), of which C-terminal end is fused with an enhanced green fluorescent protein (EGFP), named LucN-pm. The LucN-pm is located on the plasma membrane by fusing at the C-terminus of the fusion protein with a CAAX motif, which is a polybasic plasma membrane localization signal (KKKKKKSKTKCVIM) of KRas4B.<sup>2</sup> The other is a C-terminal luciferase fragment (McLuc1)<sup>1</sup> fused with a red fluorescent protein (mCherry) and tandem PH domains, designated as PP-LucC. Based on the scheme of PIP3 analysis, the LucN-pm is localized predominantly on the plasma membrane, whereas the PP-LucC is in cytosol. When PIP3 is generated on the plasma membrane, PP-LucC migrates to the plasma membrane, on which luciferase fragments are reconstituted to an active form by co-localization of PP-LucC and LucN-pm. Therefore, the change in bioluminescence signals is proportional to the amount of PP-LucC on the plasma membrane. The bioluminescence intensity indicates relative amounts of synthesized PIP3 on the plasma membrane in response to the external stimuli. Although it is difficult to measure the absolute PIP3 amount with the present system, the PIP3 probes enable to analyze quantitatively the chemicals that activate or inhibit the PIP3 production.

### 2.3.2. Validation of the Production of PIP3 in CHO-PDGFR Cell Line

In order to validate the ability of CHO-PDGFR cells to produce PIP3, immunostaining of PIP3 in vitro and translocation assay of PH domain in living cells was performed. The PIP3 immunostaining used a PIP3 antibody is shown in Figure 2-2. However, this result does not show clearly the localization of PIP3. This may be because PIP3 was washed away by the treatment of a Triton X-100 detergent, and the antibody binds non-specifically to other cellular components. On the other hand, translocation of PH domain probe in living cells is shown in Figure 2-3. In this experiment, translocation of EGFP-P upon PIP3 production in living cells was observed under a confocal microscopy. After PIP3 production stimulated by addition of PDGF, EGFP-P translocated clearly from cytosol to the plasma membrane. This result, in accordance of previous report, indicates the synthesis of PIP3 on plasma membrane.<sup>3</sup>

### 2.3.3. Characterization of the PIP3 Probes

For the promotion of effective complementation of luciferase fragments, tandem PH domains were used to enhance the stability of the PIP3 targeting probe to the PIP3. Based on structural information of a PIP3 binding protein of p42IP4 (Ins(1,3,4,5)P4/PIP3-binding protein), which contains tandem PH domains,<sup>8</sup> we inferred that the increment of PH domain numbers can enhance the PIP3 targeting efficiency. To examine the effect of tandem PH domains on its affinity, we compared dynamics of EGFP-PP with EGFP-P upon the same stimulation by analyzing time-lapse fluorescence images (Fig. 2-4). The two probes were expressed individually in CHO-PDGFR cells. Both probes were expressed uniformly in cytosol before stimulation. After the addition of PDGF (60 ng/mL), the increment of fluorescence on the plasma membrane together with the decreasing of fluorescence in cytosol were observed in both probes, demonstrating translocations of probes from the cytosol to the plasma membrane. Importantly, the probes exhibited different characteristics upon PIP3

generation. In the case of single PH domain (EGFP-P), probes targeted to the PIP3 and reached their highest efficiency 5 min after stimulation followed by marked dissociation from plasma membrane. In contrast, tandem PH domains (EGFP-PP) targeted PIP3 rapidly and then dissociated slowly from the plasma membrane. Based on this result, we conclude that tandem PH domains provide stable binding to the membrane PIP3. Such stability facilitates complementation between the split luciferase fragments.

According to the scheme for PIP3 detection, discrete localizations of PP-LucC and LucN-pm are of critical importance. We next investigated the probe localization by fluorescence imaging using a confocal microscope. Cells expressing both probes were stimulated by 20% serum, which induces PIP3 synthesis by activating the PI 3-kinase.<sup>5</sup> The probe localizations were traced with red and green fluorescent proteins, which are respectively connected with PP-LucC and LucN-pm. Before addition of serum, PP-LucC was localized in cytosol, whereas LucN-pm was exclusively on the plasma membrane. In contrast, PP-LucC migrated to the plasma membrane in response to serum stimulation, indicating that probe co-localization occurred after PIP3 production (Fig. 2-5).

#### 2.3.4. Bioluminescence Analysis of PIP3 Production

To investigate whether the probes are useful for the analysis of PIP3 production in living cells, we performed time-lapse analysis of bioluminescence by photon counting. CHO-PDGFR cells stably expressing PP-LucC and LucN-pm were generated. Then the expressions and sizes of the two fusion proteins were confirmed by Western blot analysis (Fig. 2-11). The cells were stimulated with either serum or DMEM/F-12 as a control. In addition, the effect of PI 3-kinase inhibitor, wortmannin, on PIP3 production was investigated.<sup>9</sup> The D-luciferin substrate was added before addition of the reagents. Then bioluminescence was recorded every 1 min. Bioluminescence signals of the cells

stimulated by serum increased significantly (Fig. 2-6). However, the population of the cells that pretreated with wortmannin show little response to the serum and the bioluminescence intensity remains low. Cells added with DMEM/F-12 show basal amount of PIP3. The time course of the bioluminescence signal is almost identical to that of fluorescence signal of EGFP-PP accumulated to the plasma membrane (Fig. 2-4), indicating that the recovery of bioluminescence is triggered by the PP-LucC translocation.

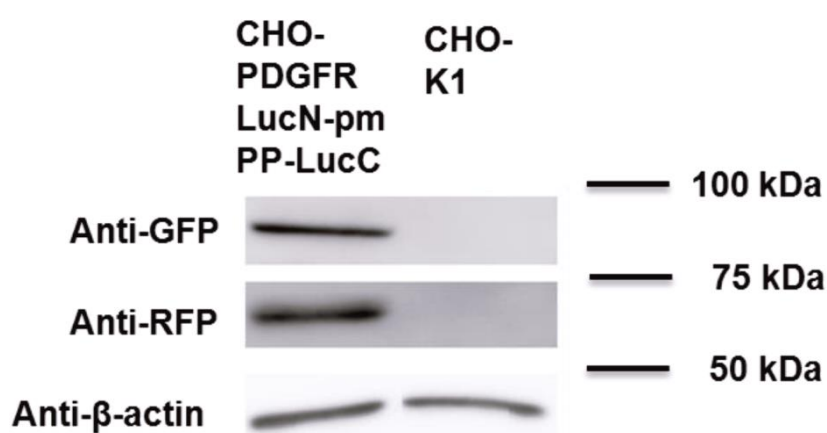


**Figure 2-11.** Western blot analysis of the probe expression. CHO-PDGFR cells expressing PP-LucC and LucN-pm were blotted respectively with anti-RFP and anti-GFP antibodies. The size range for the two probes is also shown.

To analyze the bioluminescence intensities of the spontaneously reconstituted luciferase generated from the PIP3 probes, dual bioluminescence assay using 96-well microtiter plates was performed. We examined the effects of PIP3 agonists and an inhibitor on the bioluminescence. CHO-PDGFR cells expressing the probes and RLuc were cultured in a 96-well microtiter plate and were pretreated with 0.21  $\mu\text{g}/\text{mL}$  wortmannin or DMEM/F-12 for 1 h. The cells were stimulated with 10% serum or 50 ng/mL PDGF. After the stimulation, 50  $\mu\text{L}$  Dual-Glo was added to each well for the

analysis of PIP3 production, followed by the measurement of RLuc bioluminescence. The cells stimulated by serum/PDGF generated a clearly enhanced bioluminescence compared to the control cells without addition of wortmannin or serum (Fig. 2-7). In contrast, the wortmannin pretreated cells show a suppressed bioluminescence signal. The results show that synthesis and inhibition of PIP3 are evaluated by bioluminescence signals from the PIP3 probes.

We next analyzed bioluminescence intensities of the lysed cells stimulated with PDGF, and compared the absolute bioluminescence signals with those of the live cells. The absolute intensity of bioluminescence from the lysed cells is preferably higher than that from the live cells shown in Figure 2-12.

In addition, we investigated the bioluminescence probe reversibility by the repeated stimulation and depletion of PDGF. To remove the PDGF, the buffer including PDGF was replaced by the medium without PDGF. The relative bioluminescence intensity of RLU ratio reached almost basal level 2 h after removal of PDGF, and the ratio again increased and decreased according to the addition and depletion of PDGF (Fig. 2-8).

These results demonstrate that the bioluminescent probes are useful to investigate the production and inhibition of membrane PIP3 in living cells.

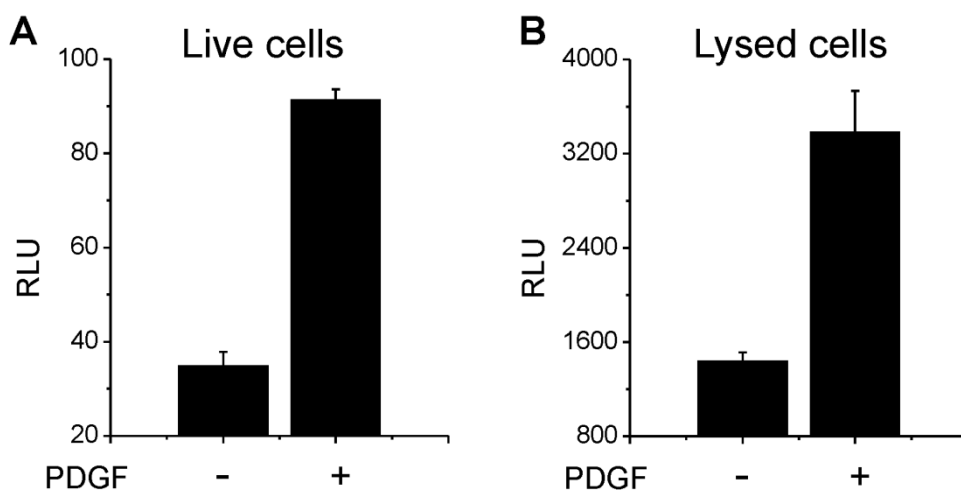


**Figure 2-12.** Comparison between bioluminescence intensities of live cells and lysed cells. CHO-PDGFR cells stably expressing PP-LucC, and LucN-pm were seeded in a 96-well microtiter plate. The cells were stimulated with PDGF (100 ng/mL) for 25 min. (A) D-luciferin (5 mM) was added to the live cells and the bioluminescence signals were acquired directly. (B) The bioluminescence signals were obtained by mixing 50  $\mu$ L Bright-Glo into each well for 5 min. (Exposure time for all measurement: 1 s, n=3)

### 2.3.5. Quantitative Analyses for PIP3 Activation and Inhibitory Effects of PIP3 Stimulants

Next, we investigated a dose-dependent effect of PDGF on the PIP3 production by the dual bioluminescence assays. Cells expressing the probes and RLuc were prepared on a 96-well microtiter plate. The cells were stimulated with PDGF in final concentrations of 0.01, 0.1, 1, 10, 50, and 200 ng/mL. Bioluminescence of the reconstituted luciferase and RLuc was measured by addition of the respective reagents. The obtained RLU ratios fit with a dose dependent curve for the PDGF concentration (Fig. 2-9A). The concentration for 50% of maximal effect ( $EC_{50}$ ) for PDGF to generate PIP3 was estimated as 3.8 ng/mL. To examine an effect of the cell lysis reagent on  $EC_{50}$

values, we investigated time-dependent dissociation of the luciferase fragments with different exposure times of lysis buffer. The buffer was added in each well and incubated from 5 to 40 min. There was almost no variation of the resulting EC<sub>50</sub> values within 20 min (Fig. 2-13). This indicates that the reagent used in the assay, although leads to the dissociation of luciferase fragments and a gradual decay of bioluminescence signal, does not affect significantly to the evaluation of EC<sub>50</sub> values. These results suggest that the bioluminescence probes are able to monitor the relative amount of PIP3 on the plasma membrane produced by stimulation of the PIP3

Next, a dose-dependent effect of PIP3 inhibitor on PIP3 production was examined using the same dual bioluminescence assays as that was used to examine the effect of PDGF. The cells expressing both probes and RLuc were preapred and were pretreated with different concentrations of wortmannin ranging from 4.3 pg/mL to 0.42 µg/mL. After 1 h pretreatment, agonist of 50 ng/mL PDGF or 10% serum was then added to all wells. The RLU ratios show the relative amount of PIP3 generated by PDGF or serum against wortmannin inhibition (Figs. 2-9B, 2-9C). In both cases of the PIP3 generated by the stimulants, bioluminescence signals show dose-dependent inhibitory effects of wortmannin. The EC<sub>50</sub> of wortmannin against PDGF was evaluated as 8.8 ng/mL, whereas EC<sub>50</sub> of wortmannin against serum was 6.1 ng/mL. A possible explanation to the lower EC<sub>50</sub> value of wortmannin against serum is that 10% serum contains lower amount of growth factor compared to the 50 ng/mL PDGF. Therefore, stimulation effects of serum are more likely to be inhibited by wortmannin. This result demonstrates that the PIP3 probes are able to analyze the PIP3 inhibitory effect in a quantitative manner. The robust assessment of PIP3 inhibition is beneficial for the screening of PIP3 inhibitors for anti-cancer drug development.

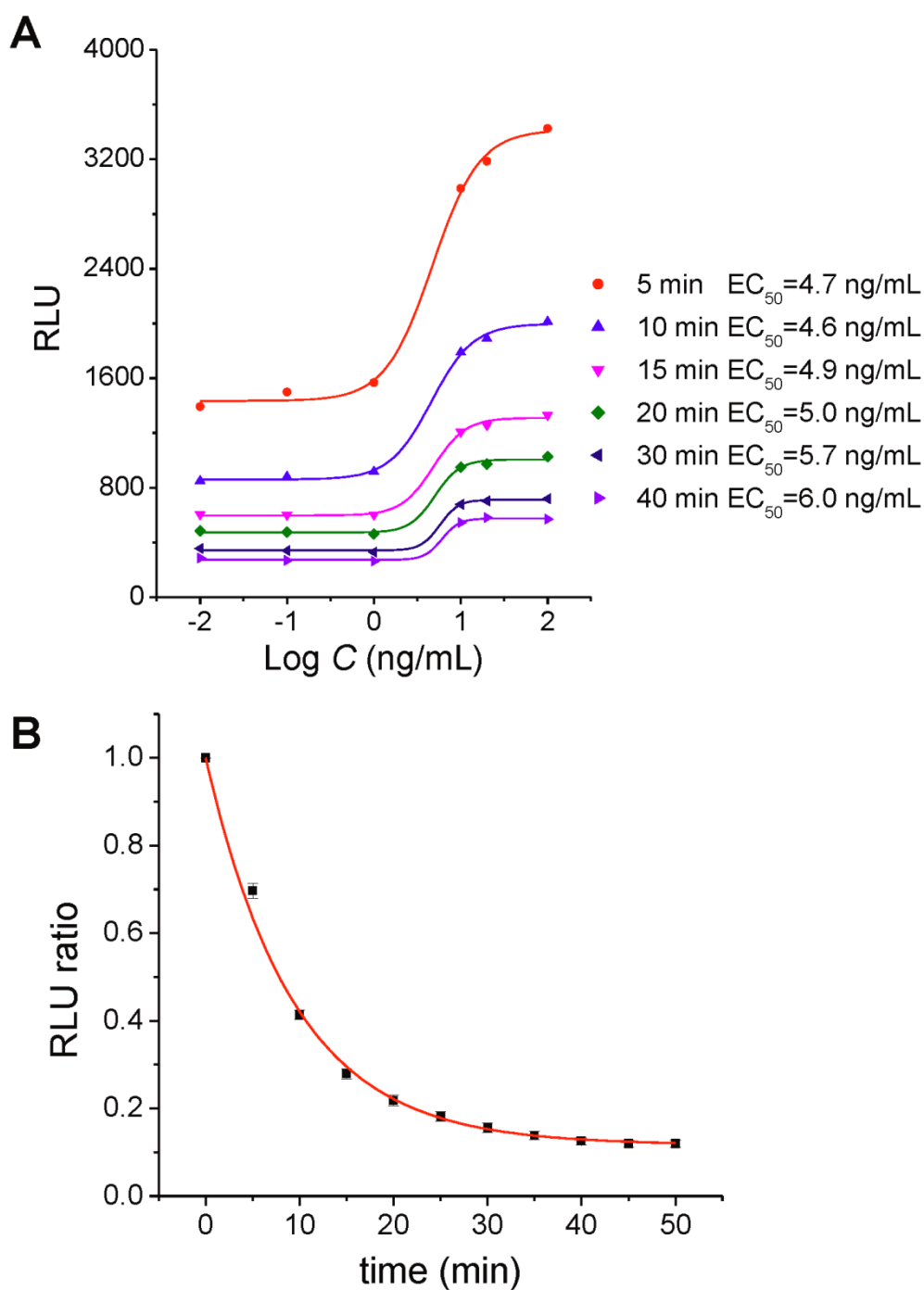


Figure 2-13. Time-dependent bioluminescence decay using the Bright-Glo lysis buffer. CHO-PDGFR cells expressing PP-LucC and LucN-pm were prepared in a 96-well microtiter plate. Different concentrations of PDGF were added into each well. After the PDGF stimulation, cells were incubated with the 50  $\mu$ L Bright-Glo buffer with different durations (Exposure time, 1 s). (A) Dose-dependent curves of bioluminescence intensities with incubation times from 5 min to 40 min of the Bright-Glo lysis buffer. Obtained  $EC_{50}$  values are shown. (B) Time-dependent exponential decay of bioluminescence signals indicating the dissociation of luciferase fragments within 50 minutes.

### 2.3.6. Application to a HTS System

The aberrant amount of PIP3 has fatal impacts on living organisms. Reagents that affect PIP3 amount may become valid candidates for the drug development. Our PIP3 probes are able to analyze the relative PIP3 amount in a cell population. Therefore, a promising application is to identify chemicals that control PIP3 production with a HTS system. To demonstrate the applicability of the probes for the HTS, we validated an assay system with the probes on 96-well microtiter plates. Cells expressing the PIP3 probes were subjected to bioluminescence assays using a 96-well microtiter plate reader. We used the flanking wells of a plate on both sides as negative controls and the remainder of the wells as positive controls. The cells in each well were activated using 10% serum as an agonist. Inhibition assays were conducted using 86 ng/mL wortmannin as an inhibitor. Bioluminescence signals of entire microtiter plates upon stimulation with the agonist or upon stimulation of agonist against inhibitor pretreatment are presented in Figure 2-14. Based on the heat maps of agonist screening (Fig. 2-15A), we calculated the average bioluminescence intensities of activation and negative control wells. An intensity distribution map was also obtained (Fig. 2-14A), from which  $Z'$  factor of 0.65 was estimated. The result demonstrates that the probes are applicable for effective HTS of PIP3 agonist. In addition, the heat map of PIP3 inhibition assays (Fig. 2-15B), the average bioluminescence intensities of inhibition and negative control wells and signal distribution map were obtained (Fig. 2-14B). The  $Z'$  factor of the inhibition assay is 0.73, which indicates separation of inhibitory and non-inhibitory effects. Such separation validates the applicability of the PIP3 probes for high throughput screening of PIP3 inhibitor.

### 2.3.7. Imaging of PIP3 Production using a Bioluminescence

## Microscope

A salient benefit of bioluminescence assay is its ability to elucidate biological events in living cells with minimal damage to the cells. We performed live cell bioluminescence imaging with the PIP3 probes to visualize the production of PIP3. D-Luciferin was added to the culture medium before observations. The bioluminescence and differential interference contrast (DIC) images were acquired, respectively, with exposure times of 10 min and 300 ms (Fig. 2-10). Cells expressing the PIP3 probes were stimulated by 10% serum. When we compared images before and after stimulations, marked enhancement of bioluminescence was observed. This result suggests that the PIP3 production in living cells was visualized using bioluminescent probes.

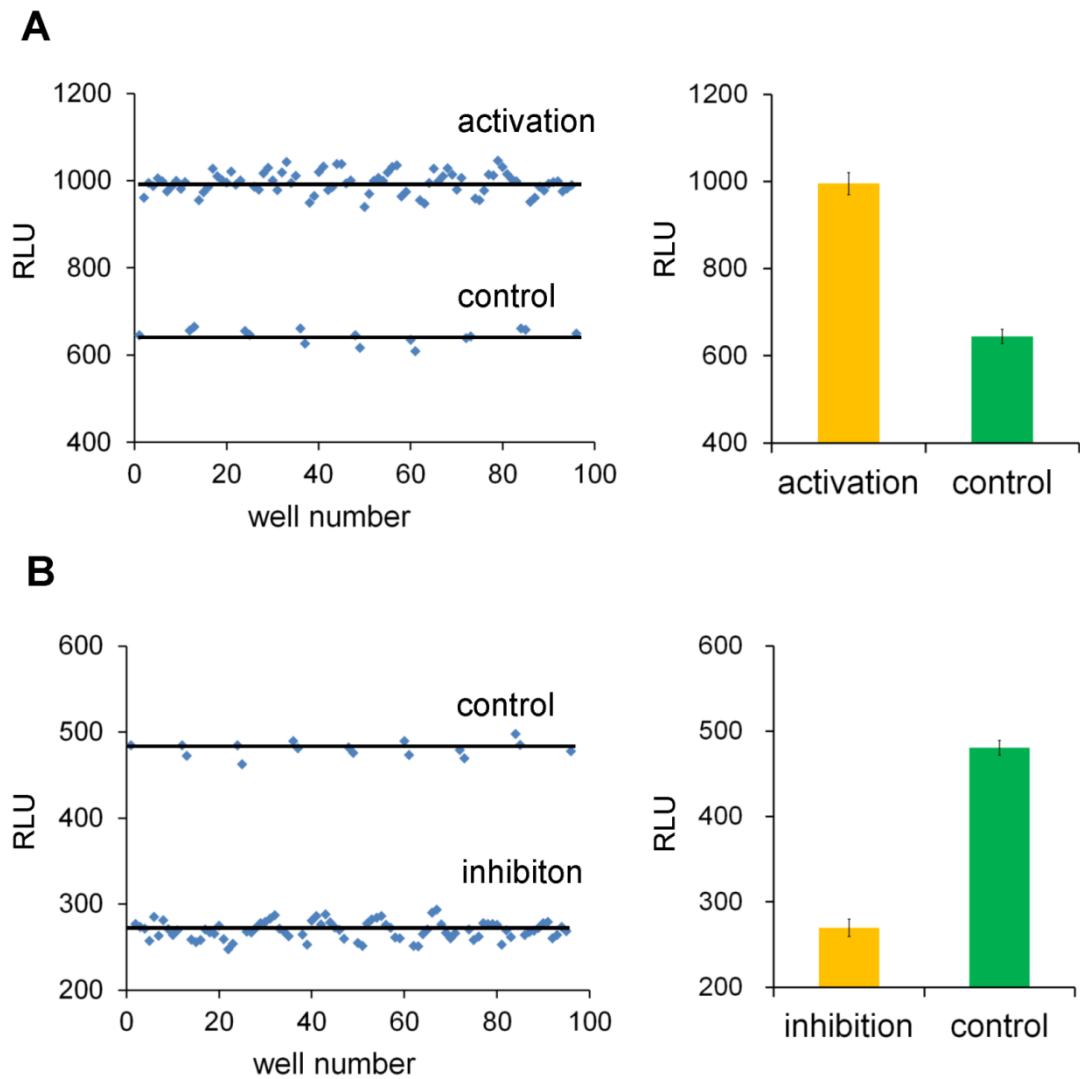


**Figure 2-14.** Validation of a high-throughput screening system for PIP3-regulation-compound. Cells stably expressing LucN-pm and PP-LucC were subcultured into a 96-well microtiter plate. The middle 80 wells of the plate were used for positive controls and the flanking 16 wells were for negative controls. The bioluminescence signals of all wells after stimulation are shown as a distribution map and average intensities. (A) Validation of the PIP3 agonist HTS system. Positive control wells (activation) were stimulated with 10% serum, whereas negative control wells (control) were added with DMEM/F-12. The estimated  $Z'$  factor is 0.65. (B) Validation of PIP3 inhibitor HTS system. Positive control wells (inhibition) were pretreated with 86 ng/mL wortmannin and negative control wells (control) were pretreated with DMEM/F-12. All wells were then activated by 10% serum. The  $Z'$  factor for the inhibitor screening system is 0.73.

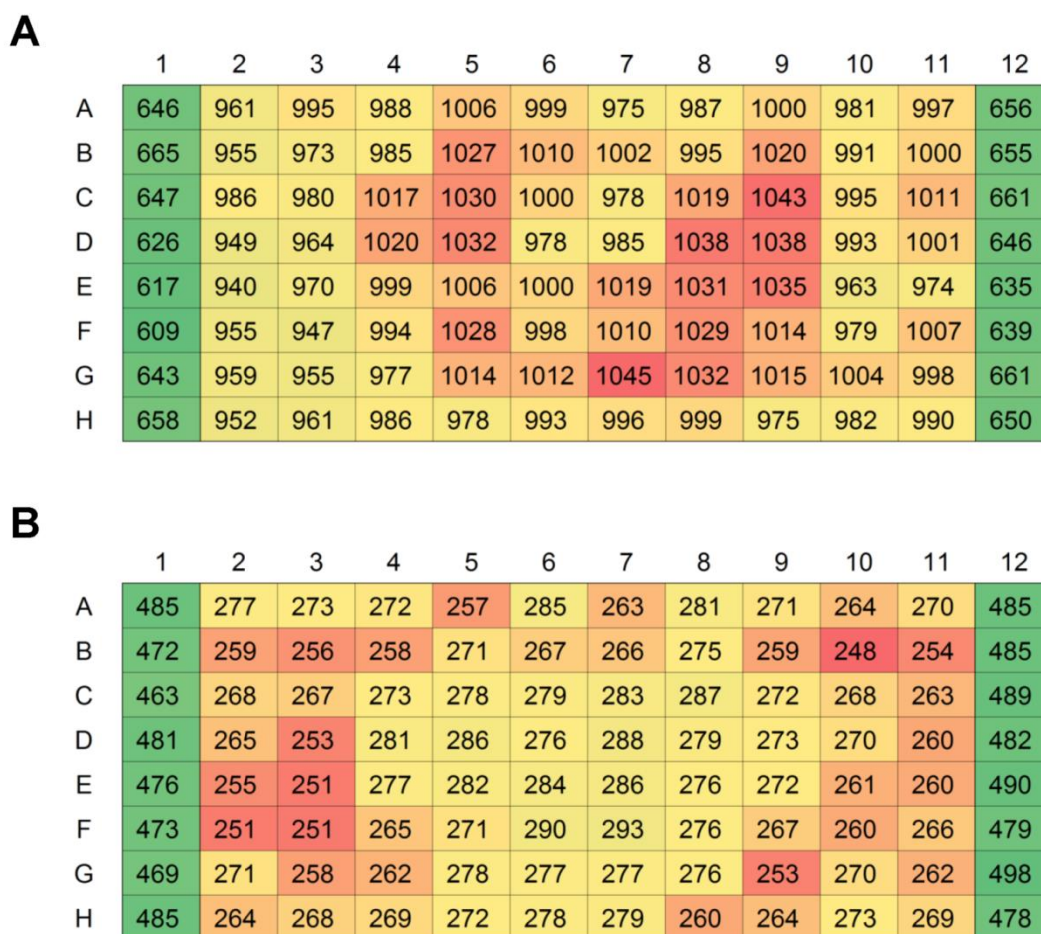


**Figure 2-15.** Heat maps for the validation of HTS. Cells stably expressing LucN-pm and PP-LucC were subcultured into a 96-well microtiter plate and were subjected to evaluation for drug screening by comparing positive and negative controls. The RLU of all wells after stimulation are shown as a heat map. Green denotes negative control wells, whereas yellow and red stand for positive control wells. The average intensity (Av), coefficient of variation (CV), signal to background ratio (S/B), and Z' factor were calculated. (A) Validation of PIP3 agonist HTS by serum: Av(+)=995.30, CV(+)=2.50%, Av(-)=644.73, CV(-)=2.51%, S/B=1.54, and Z' factor=0.65. (B) Validation of PIP3 inhibitor HTS by wortmannin: Av(+)=269.59, CV(+)=3.81%, Av(-)=480.58, CV(-)=1.80%, S/B=0.56, and Z' factor=0.73.

## 2.4. Discussion

In this study, a pair of bioluminescent probes for PIP3 analysis based on luciferase fragment complementation was developed. The existing in-vitro and in-vivo methods exhibit bottle-neck problems in the analysis of relative PIP3 amounts because of the fast dynamic property of PIP3 and the presence of its analogues. We successfully overcame these issues by combining the use of PH domain as a PIP3 recognition module with the split-luciferase complementation technology. In addition, the detection scheme of self-associative fragment complementation is novel; co-localization of the LucN-pm and PP-LucC enables complementation of the luciferase fragments into an active form. In previous methods, fragments of split luciferase were brought into proximity by two mechanisms: One is intramolecular complementation, which is triggered by a conformational change of a protein. The other is intermolecular complementation, which occurs from protein-protein interactions. In both cases, enforced interaction between split fragments is a prerequisite for bioluminescence recovery. Our PIP3 probes are designed conceptually to use an increase in local concentration of probes on the plasma membrane, causing self-complementation of luciferase fragments on plasma membrane after the production of PIP3 (Fig. 2-1). For sensitive analysis, we demonstrated that tandem PH domains enhance its interaction with PIP3, resulting in the recovery of higher bioluminescence. Moreover, two important features are necessary for the luciferase complementation: i) co-localization of complementary fragments with an appropriate orientation and ii) moderate affinity between the two fragments. Co-localization of PP-LucC and LucN-pm is confirmed by the fluorescence images (Fig. 2-5) and the right orientation of luciferase fragments is facilitated by flexible linker in the fusion protein. The latter feature of moderate affinity between CBRN and McLuc1 has been demonstrated in a previous report.<sup>1</sup> This novel self-association scheme broadens the application of luciferase fragment

complementation into different kinds of lipids and signaling molecules.

We demonstrated that the designed probes enabled the evaluation of the PIP3 production with bioluminescence signals. Studies using bioluminescent probes have been reported for the analysis of second messengers such as cAMP,<sup>10,11</sup> calcium,<sup>12</sup> and IP3.<sup>13</sup> These second messengers are water-soluble molecules dispersed in the cytoplasm. Such molecules are analyzed based on their downstream effector proteins. Their conformational changes are converted into bioluminescence signals that reflect the relative concentrations of the signal molecule. In contrast, a bottle-neck impeded the analysis of PIP3 on the plasma membrane. The PH domain undergoes no conformational change upon binding with PIP3.<sup>14</sup> We therefore approached bridging the methodological gap, and analyzed the relative PIP3 amount using a self-associative luciferase fragment complementation. The relative PIP3 amount is indicated by absolute photon counting of complemented luciferase from the cell population. We interpreted the effect of PIP3 production and inhibition with a quantitative bioluminescence signal. Furthermore, the concentration dependence of the agonist and inhibitor for PIP3 production was analyzed using these probes.

We applied the designed probes to the establishment of a HTS system for PIP3 agonists and antagonists. An excessive amount of PIP3 is involved in tumorigenic signaling pathways. Depletion of PIP3 contributes to developmental failure and retards nerve cell growth.<sup>15,16</sup> Fluorescent proteins have their limitations on the screening project because, in the presence of excitation light, the intrinsic fluorescence of library chemicals is prone to producing false positive results. In addition, previous PIP3 analyses using fluorescence-based technology exhibit major shortcomings of cell damage produced by the laser that is used for fluorescent protein excitation. In comparison to fluorescence technology, bioluminescence is advantageous for drug screening because bioluminescence exhibits little interference with fluorescence of

library chemicals. This method compensates for the shortcomings of the toxicity of laser light. The established cell line in the present study showed dynamic changes of bioluminescence signals because the cell produced sufficient amounts of PIP3 on the plasma membrane upon extracellular stimulation. This cellular property is necessary for the development of a screening system. In fact, we have obtained  $Z'$  factors higher than 0.5, which indicates a valid screening system,<sup>7</sup> in both PIP3 agonist and inhibitor screening evaluations using the probes (Fig. 2-15). Such a system is suitable for systematic and automated HTS of PIP3 control compounds as primary screening.

## 2.5. Conclusion

In conclusion, we developed probes for PIP3 analysis based on luciferase fragment complementation. Then we introduced the novel concept of self-associative luciferase fragment complementation for PIP3 analysis. The PIP3 probes provide important features including temporal recording of PIP3 production by bioluminescence and analysis of relative PIP3 amounts with minimal cell toxicity. We quantified agonist and inhibitor of PI 3-kinase that affected production of PIP3 on the plasma membrane. This approach clarifies a path to more extensive investigation of membrane lipid second messenger using luciferase fragment complementation. Other PIs that play distinctive roles in cells can as well be analyzed by replacing PIP3 targeting PH domain (GRP1) with other PI targeting motifs. Systematic analysis of PIs in different cell organelles will be undertaken to investigate the diverse functions of PIs to reveal complex lipid signaling networks in the future.

## 2.6. Reference

1. Hida, N.; Awais, M.; Takeuchi, M.; Ueno, N.; Tashiro, M.; Takagi, C.; Singh, T.; Hayashi, M.; Ohmiya, Y.; Ozawa, T. *PLoS ONE* **2009**, *4* (6), e5868.
2. Kennedy, M. J.; Hughes, R. M.; Peteya, L. A.; Schwartz, J. W.; Ehlers, M. D.; Tucker, C. L. *Nat. Meth.* **2010**, *7* (12), 973-975.
3. Oatey, P. B.; Venkateswarlu, K.; Williams, A. G.; Fletcher, L. M.; Foulstone, E. J.; Cullen, P. J.; Tavaré, J. M. *Biochem. J.* **1999**, *344* (2), 511-518.
4. Kazlauskas, A.; Cooper, J. A. *EMBO J.* **1990**, *9* (10), 3279.
5. Zhang, H.; Bajraszewski, N.; Wu, E.; Wang, H.; Moseman, A. P.; Dabora, S. L.; Griffin, J. D.; Kwiatkowski, D. J. *J. Clin. Invest.* **2007**, *117* (3), 730-738.
6. Takakura, H.; Hattori, M.; Takeuchi, M.; Ozawa, T. *ACS Chem. Biol.* **2012**, *7* (5), 901-910.
7. Zhang, J.; Chung, T. D.; Oldenburg, K. R. *J. Biomol. Screen.* **1999**, *4* (2).
8. Sedehizade, F.; Hanck, T.; Stricker, R.; Horstmayer, A.; Bernstein, H.-G.; Reiser, G. *Brain. Res. Mol. Brain Res.* **2002**, *99* (1), 1-11.
9. Yano, H.; Nakanishi, S.; Kimura, K.; Hanai, N.; Saitoh, Y.; Fukui, Y.; Nonomura, Y.; Matsuda, Y. *J. Biol Chem.* **1993**, *268* (34), 25846-25856.
10. Takeuchi, M.; Nagaoka, Y.; Yamada, T.; Takakura, H.; Ozawa, T. *Anal. Chem.* **2010**, *82* (22), 9306-9313.
11. Stefan, E.; Aquin, S.; Berger, N.; Landry, C.; Nyfeler, B.; Bouvier, M.; Michnick, S. *Proc. Natl. Acad. Sci. U. S. A.* **2007**, *104* (43), 16916-16921.
12. Saito, K.; Hatsugai, N.; Horikawa, K.; Kobayashi, K.; Matsu-ura, T.; Mikoshiba, K.; Nagai, T. *PLoS ONE* **2010**, *5* (4), e9935.
13. Ataei, F.; Torkzadeh-Mahani, M.; Hosseinkhani, S. *Biosens. Bioelectron.* **2013**, *41*, 642-648.
14. Lietzke, S. E.; Bose, S.; Cronin, T.; Klarlund, J.; Chawla, A.; Czech, M. P.; Lambright, D. G. *Mol. Cell* **2000**, *6* (2), 385-394.
15. Skwarek, L. C.; Boulianne, G. L. *Dev. cell* **2009**, *16* (1), 12-20.

16. Ménager, C.; Arimura, N.; Fukata, Y.; Kaibuchi, K. *J. Neurochem.* **2004**, *89* (1), 109-118.

### 3.Optical Control of PIP3 Production on Cell Membranes

#### 第3章

本章については、5年以内に雑誌等で刊行予定のため、非公開。

## 4. General Conclusion

In this thesis, developments of novel methods for the analysis of PIP3 are established. PIP3 is an important molecule that mediates diverse cellular functions. Current analytical methods for PIP3 studies are insufficient to further analyze the detail of PIP3 signaling and amounts. The previous *in vitro* methods suffer from sample pretreatment and fluorescence *in vivo* imaging fails to spatiotemporally analyze the PIP3 amount. To solve these problems and limitations, bioluminescent probes were developed for the analyses of relative PIP3 amounts on the plasma membrane. The monitoring of PIP3 production on the plasma membrane by light regulation was also demonstrated.

In Chapter 2, a bioluminescent probe for PIP3 detection using split luciferase complementation was demonstrated. In this probe, an N-terminal fragment of a luciferase is predominantly localized on the plasma membrane, whereas a C-terminal fragment of a luciferase fused with a PH domain from GRP1, which specifically targets the PIP3, is expressed in the cytosol. A novel mechanism of self-associative luciferase complementation is introduced by our split luciferase probes, which are on the basis of an increase in the local concentration of both probes as a driving force for luciferase-fragment complementation. After the production of PIP3, the co-localization of N- and C-terminal luciferases on the plasma membrane cause self-associative complementation of the luciferase fragments on plasma membrane. Using this probe, we successfully conveyed PIP3 levels to quantitative bioluminescence signals and quantified the relative PIP3 amounts produced by specific agonists. We have also applied the probe to a high-throughput screening platform. Unlike fluorescence technologies, little interference existed between screening compounds with the luciferase signals. A false positive compound may lead to laborious work from cell

experiments to animal model experiments. The low background of bioluminescence assays is a strong advantage of the luciferase system compared to the fluorescence technologies, therefore, the PIP3 probes are strong tools for the drug discovery. By testing the cellular bioluminescence, it is possible to screen for a candidate that enhances or inhibits PIP3 production with high efficiency, and a series of evaluations for the drug effects can be performed. In addition, PIP3 molecules have been, for the first time, visualized by bioluminescence in living cells using a bioluminescence microscopy.

In Chapter 3 of this study, an optogenetic system using the light gated *Arabidopsis* a cryptochrome 2 (CRY2) and CIB1 interaction was established for the control of PIP3 synthesis. Upon light irradiation, spatiotemporal regulation of the PIP3 synthesis was achieved in live cells. The established optical system enables the light gated PIP3 generation in a subcellular level. The fast and reversible interaction of CRY2 and CIB1 facilitates the manipulation of PIP3 production in living cells by blue light. Directional cell movements were also induced towards or oppose other cells. This approach will be applicable for further investigation of PIP3 functions in a subcellular level.

In summary, this study introduced two analytical methods for PIP3: the detection of PIP3 by a bioluminescent probe and the control of PIP3 production using optogenetic control. The bioluminescent probes developed in this study enable detection of PIP3 by bioluminescence with spatiotemporal precision; this method involves the introduction of a conceptually-novel mechanism for luciferase fragment complementation, and provides a platform for PIP3 related compound screening which is able to promote the advancement of drug development. By using a targeting motif of another membrane signal molecule, this detection mechanism is easily adopted to analyze other biomolecules on the cell membrane by replacing the PIP3 targeting motif to a PIP2 targeting one. The optical control of PIP3 production is a strong tool to analyze PIP3

functions because it breakthroughs the bottle-neck of conventional chemical stimulations and enables spatiotemporal control of PIP3 synthesis. It enables accurate monitoring of PIP3 only on the plasma membrane, which is extremely difficult by conventional methods. In the future, further investigation of PIP3 production on endomembrane is an attractive direction. The concept of controlling lipid messengers can also be adapted to control other signaling molecules that are produced on the cell membrane. In conclusion, these studies have not only established methods to detect or control one biomolecule, the methodology is widely applicable to other biomolecules, enabling to broaden scientific understanding of membrane signaling molecules, as well as opening a clear path towards practical investigation of signaling related applications.

# Acknowledgements

I would like to express my deepest gratitude to Prof. Takeaki Ozawa, for his outstanding support and encouragement. His continuous advice and warm attitude helped me immensely as I advanced in this thesis work.

I would like to thank all committee members, Prof. Mitsuhiko Shionoya, Prof. Hiroshi Nishihara, Prof. Hiroaki Suga, and Prof. Moritoshi Sato, for their patient readings of this dissertation and insightful advices on it.

My deep appreciation goes to Dr. Mitsuru Hattori, Dr. Hideaki Yoshimura, Dr. Hideo Takakura, and Dr. Akira Kanno, who kindly offered discussions and instructions on my experiments.

My thanks as well go to former and current members of Analytical Chemistry Laboratory. They warmly offered encouragements on my research, as well as cares on my daily life. I especially would like to thank Mr. Yusuke Nasu, for having taught me experimental protocols at the earliest stage of my research and helping me when I encountered difficulties. I sincerely appreciate Ms. Saori Hashiguchi, Ms. Qiaojing Li, Ms. Ayari Takamura, Mr. Toshimichi Yamada, Mr. Keiichiro Kitada, Mr. Yoshihiro Katsura, and Mr. Mizuki Endo. The friendship from each of them made my life in the lab so joyful and filled with warm memories.

I feel also grateful to my other friends in Japan. Dr. Bangan Liu had advised me to prepare materials for the entrance of the University of Tokyo; Ms. Na Xu had helped me after the 3.11 earthquake; Dr. Yongwei Xu had invited me to play violin together. Dr. Jing Zhang had offered insightful discussions on my research and took care of me when I was ill. Dr. Shu Liu had invited me to the Japanese courses. I am very sorry that I could not list all of their names here, but each of friendships I harvested in Japan is a precious gift to me which I will cherish for life.

Finally, I also thank my parents and my husband who have always supported and believed in me during my Ph. D. course.